Calhoun: The NPS Institutional Archive

DSpace Repository

Theses and Dissertations | 1. Thesis and Dissertation Collection, all items

1987-03

Representation of nonstationary narrowband random processes and their application and effectiveness as jamming signals in spread spectrum communication systems

Low, Kah Meng

http://hdl.handle.net/10945/22458

Copyright is reserved by the copyright owner

Downloaded from NPS Archive: Calhoun

http://www.nps.edu/library

Calhoun is the Naval Postgraduate School's public access digital repository for research materials and institutional publications created by the NPS community. Calhoun is named for Professor of Mathematics Guy K. Calhoun, NPS's first appointed -- and published -- scholarly author.

Dudley Knox Library / Naval Postgraduate School
411 Dyer Road / 1 University Circle
Monterey, California USA 93943

DUDLEY KNOX LIBRARY
NAVAL POSTGRADUATE SCHOOL
MONTEREY CALIFORNIA 93943-5002

NAVAL POSTGRADUATE SCHOOL
Monterey, California

THESIS

REPRESENTATION OF NONSTATIONARY NARROWBAND RANDOM PROCESSES AND THEIR APPLICATION AND EFFECTIVENESS AS JAMMING SIGNALS IN SPREAD SPECTRUM COMMUNICATION SYSTEMS

by

Kah Meng, Low

March 1987

Thesis Advisor: Daniel Bukofzer

Approved for public release; distribution is unlimited

T233136

UNCLASSIFIED
ECURITY CLASSIFICATION OF THIS PAGE

REPORT DOCUMENTATION PAGE

a REPORT SECURITY CLASSIFICATION UNCLASSIFIED	1b RESTRICTIVE MARKINGS
a SECURITY CLASSIFICATION AUTHORITY	3 DISTRIBUTION/AVAILABILITY OF REPORT Approved for public release; distribution is unlimited
b DECLASSIFICATION / DOWNGRADING SCHEDULE	
PERFORMING ORGANIZATION REPORT NUMBER(S)	5 MONITORING ORGANIZATION REPORT NUMBER(S)
a NAME OF PERFORMING ORGANIZATION Naval Postgraduate School	6b OFFICE SYMBOL (If applicable) Code 62
7a NAME OF MONITORING ORGANIZATION Naval Postgraduate School	
: ADDRESS (City, State, and ZIP Code) Monterey, California 93943-5002	7b ADDRESS (City, State, and ZIP Code) Monterey, California 93943-5002
a NAME OF FUNDING / SPONSORING ORGANIZATION	8b OFFICE SYMBOL (If applicable)
9 PROCUREMENT INSTRUMENT IDENTIFICATION NUMBER	
ADDRESS (City, State, and ZIP Code)	10 SOURCE OF FUNDING NUMBERS

PROGRAM ELEMENT NO	PROJECT NO	TASK NO	WORK UNIT ACCESSION NO

TITLE (Include Security Classification)
REPRESENTATION OF NONSTATIONARY NARROWBAND RANDOM PROCESSES AND THEIR APPLICATION AND EFFECTIVENESS AS JAMMING SIGNALS IN SPREAD SPECTRUM COMMUNICATION SYSTEMS

PERSONAL AUTHOR(S)
LOW, Kah Meng

a TYPE OF REPORT	13b TIME COVERED	14 DATE OF REPORT (Year, Month Day)	15 PAGE COUNT
Master's Thesis	FROM _____ TO _____	1987, March	91

SUPPLEMENTARY NOTATION

COSATI CODES			18 SUBJECT TERMS (Continue on reverse if necessary and identify by block number)
FIELD	GROUP	SUB-GROUP	nonstationary random processes; spread spectrum communication; pulsed noise jammer

ABSTRACT (Continue on reverse if necessary and identify by block number)

A representation of nonstationary narrowband random processes in terms of nonstationary quadrature components is proposed in a form analogous to that used to represent wide sense stationary narrowband random processes. The representation is then applied to a specific case in which the nonstationary narrowband random process is generated by the product of white noise and a deterministic periodic signal and then is processed by a narrowband filter. This representation is used in the modeling of a bi-level pulsed noise jammer which is assumed to be present in a communication channel. The effect of such a jammer on a direct sequence, binary phase shift keyed (DS-BPSK) spread spectrum communication receiver is evaluated and characterized in terms of the error rate performance of the receiver. Families of performance curves are plotted to demonstrate the effect of various parameters, namely signal-to-noise ratio, jammer power to signal power ratio, and processing gain, on the error rate of the complete spread spectrum receiver. The analysis carried out differentiates between two cases, namely fast jammers and slow jammers. However, the analytical tools developed make it possible to consider either one of the two cases without resorting to quasi-stationary arguments as has been done in the past.

DISTRIBUTION / AVAILABILITY OF ABSTRACT	21 ABSTRACT SECURITY CLASSIFICATION
☒ UNCLASSIFIED/UNLIMITED ☐ SAME AS RPT ☐ DTIC USERS	UNCLASSIFIED

NAME OF RESPONSIBLE INDIVIDUAL	22b TELEPHONE (Include Area Code)	22c OFFICE SYMBOL
Prof. Daniel Bukofzer	(408) 646-2859	Code 62Bh

FORM 1473, 84 MAR 83 APR edition may be used until exhausted
All other editions are obsolete

SECURITY CLASSIFICATION OF THIS PAGE
UNCLASSIFIED

Approved for public release; distribution is unlimited

Representation of Nonstationary Narrowband Random Processes and their Application and Effectiveness as Jamming Signals in Spread Spectrum Communication Systems

by

Kah Meng, Low
Ministry of Defense, Singapore
Diplôme d'Ingénieur. ESME Paris, 1980

Submitted in partial fulfillment of the
requirements for the degree(s) of

MASTER OF SCIENCE IN ELECTRICAL ENGINEERING

from the

NAVAL POSTGRADUATE SCHOOL
March 1987

ABSTRACT

A representation of nonstationary narrowband random processes in terms of nonstationary quadrature components is proposed in a form analogous to that used to represent wide sense stationary narrowband random processes. The representation is then applied to a specific case in which the nonstationary narrowband random process is generated by the product of white noise and a deterministic periodic signal and then is processed by a narrowband filter. This representation is used in the modeling of a bi-level pulsed noise jammer which is assumed to be present in a communication channel. The effect of such a jammer on a direct sequence, binary phase shift keyed (DS-BPSK) spread spectrum communication receiver is evaluated and characterized in terms of the error rate performance of the receiver. Families of performance curves are plotted to demonstrate the effect of various parameters, namely signal-to-noise ratio, jammer power to signal power ratio, and processing gain, on the error rate of the complete spread spectrum receiver. The analysis carried out differentiates between two cases, namely fast jammers and slow jammers. However, the analytical tools developed make it possible to consider either one of the two cases without resorting to quasi-stationary arguments as has been done in the past.

TABLE OF CONTENTS

I. INTRODUCTION 8

II. NONSTATIONARY RANDOM PROCESSES 11

A. NONSTATIONARY NARROWBAND RANDOM PROCESSES 11

1. Lowpass Equivalent of a Narrowband Filter 12

2. Output of a Narrowband Filter 14

3. Output Correlation Function for Nonstationary Input 16

B. A MODEL FOR THE NONSTATIONARY INPUT 17

C. A SPECIFIC EXAMPLE 19

III. EFFECT OF SPREAD SPECTRUM SYSTEM ON NON-STATIONARY NOISE 24

A. MODEL FOR THE SPREAD SPECTRUM RECEIVER 24

B. EFFECT OF NONSTATIONARY NOISE ON THE DESPREADER AND BIT DETECTOR 27

1. Variance σ_J^2 for the Fast Jammer 30

2. Variance σ_J^2 for the Slow Jammer 31

IV. PERFORMANCE OF THE SPREAD SPECTRUM COMMUNICATION SYSTEM 34

A. GENERAL OUTLINE 34

B. RECEIVER PERFORMANCE FOR BPSK MODULATION . . 35

C. ANALYSIS OF ERROR PERFORMANCE 41

V. CONCLUSIONS 51

APPENDIX A: REPRESENTATION OF NARROWBAND FILTER . . 53

APPENDIX B: OUTPUT OF A NARROWBAND FILTER 55

APPENDIX C: NARROWBAND PROCESSES AUTOCORRELATION FUNCTION EXAMPLE 58

APPENDIX D: AUTOCORRELATION FUNCTION AND AVERAGE POWER AT THE OUTPUT 60

APPENDIX E: VARIANCE OF Y_J 66

APPENDIX F: THE EXPONENTIAL FOURIER SERIES OF $q_e(t)$ AND AVERAGE POWER OF THE PULSED JAMMER . . 73

APPENDIX G: VARIANCE σ_J^2 FOR FAST JAMMER 77

APPENDIX H: STATISTICS OF Y_J AND N_{th} 83

LIST OF REFERENCES 89

INITIAL DISTRIBUTION LIST 90

LIST OF FIGURES

2.1 Graphic Representation of $H_L(f)$ and $H_B(f)$ 13

2.2 Narrowband Filtering of Real Input $X(t)$ 15

2.3 Nonstationary Input $X(t)$ 18

2.4 Schematic Representation of the Bi-level Jammer Model 21

2.5 Functions $q(t)$ and $q_s(t)$ 22

3.1 BPSK Spreading Code $c(t)$ 25

3.2 Simplified DS-BPSK Spread Spectrum Receiver 26

3.3 Simplified DS-BPSK Spread Spectrum for Nonstationary Narrowband Input 28

3.4 Functions $P_c(f)$ and $P_c(f - nR_q)$ 32

4.1 DS-BPSK Spread Spectrum Receiver 36

4.2 Power Spectral Density of the Thermal Noise 38

4.3 Signal Space Diagram for BPSK Modulation 40

4.4a P_b Versus JSR for $G_c = 10$ 43

4.4b P_b Versus JSR for $G_c = 100$ 43

4.4c P_b Versus JSR for $G_c = 200$ 44

4.4d P_b Versus JSR for $G_c = 400$ 44

4.5a P_b Versus JSR for $SNR = 0$ dB 46

4.5b P_b Versus JSR for $SNR = 4$ dB 46

4.5c P_b Versus JSR for $SNR = 16$ dB 47

4.5d P_b Versus JSR for $SNR = 20$ dB 47

4.6a P_b Versus SJR for $G_c = 10$ 48

4.6b P_b Versus SJR for $G_c = 100$ 48

4.6c P_b Versus SJR for $G_c = 200$ 49

4.6d P_b Versus SJR for $G_c = 400$ 49

D.1 Function $[r] - [s]$ 63

D.2 Function $(t - T_q[r])$ 64

D.3 Function $(t - t_q[s])$ 65

E.1 Autocorrelation Function and Power Spectral Density for DS-BPSK Spreading Code 67

F.1 Function $q_s(t)$ 74

H.1 Function $Z'(f)$ 87

I. INTRODUCTION

Electronic Counter Measure (ECM) techniques have gained increasing attention in military communications. It is often necessary and important to be able to analyze and predict the performance of communication receivers, especially when operating under hostile electronic interference. In order to improve the survivability of tactical communication systems operating in jamming enviornments, spread spectrum modulation techniques have been introduced, analyzed and implemented in many systems in order to mitigate the effects of intentional electronic interference. In many of the analyses carried out to date, the jammer interference is typically assumed to be a stationary (or wide sense stationary) random process with well-specified statistical characterizations [Ref 1], and the natural interference introduced in the communication channel is generally modeled as additive white Gaussian noise (AWGN). However, in practice, there are many communication environments which do not fit the model just described. Consider, for example, a communication system which is being jammed by a continuous wave (CW) tone near the transmitter operating center frequency, or by a distorted retransmission of the transmitter's own signal. The interference cannot be accurately modeled as a stationary random process in either case. Another typical jamming scenario involves a jamming signal that may be pulsed between various power levels at a rapid rate and is therefore not stationary [Ref 2].

The effects of nonstationary interference on the performance of a spread spectrum communication system is not known in general. It is however possible in many cases to characterize nonstationary interferers and determine their effect on specific communication systems. In fact, if the statistics of the nonstationary

process are periodic, such a process is said to be cyclostationary [Ref. 3]. The statistics and power spectrum of a cyclostationary process are normally computed by using phase randomization or time averaging techniques [Ref. 3].

In view of the importance of the use of nonconventional forms of generating channel interference, the aim of this thesis is to analyze the effects of nonstationary narrowband interference on the performance of a spread spectrum communication receiver. More specifically, the results of the analysis are applied to the special case of a narrowband bi-level pulsed noise jammer, since it is an effective form of ECM [Ref 3]. Although certain results concerning the same type of jammer considered here can be obtained by other methods [Reference 1 and 2] the results derived are based on the application of quasi-stationary assumptions which oftentimes are not realistic and cannot always be justified in practice.

In Chapter II of the thesis, methods analogous to those used in the representation of narrowband random processes are used to characterize a stationary narrowband nonstationary random process. Such a random process is shown to be specified in terms of its nonstationary quadrature components. The expression of the autocorrelation function of the nonstationary narrowband random process is then established, and, all the results are used to specify the characterization of a bi-level, narrowband pulsed noise jammer which can be obtained by amplitude modulation of white Gaussian noise which is filtered by a narrowband filter centered at some high frequency f_0.

In Chapter III, analysis was carried out in order to characterize the output of the spread spectrum receiver consisting of a despreader, a bandpass filter and a correlation detector, when a nonstationary narrowband process is applied at the input of such a receiver. This characterization is obtained in terms of the mean

and variance of the Gaussian random variable at the output of the receiver's decision circuitry.

Chapter IV provides a detailed analysis of the performance of a spread spectrum receiver. The binary phase shift keyed (BPSK) modulation scheme was selected as the method by which digital information is transmitted and the method of spreading the signal bandwidth was chosen to be a direct sequence spread spectrum modulation approach. Noise and jamming were assumed to be sources of channel interference, using the models developed in Chapter 3 for their characterization. The receiver performance specification was accomplished by deriving the error probability or the bit error rate. The error performance was plotted versus various factors that take into account signal power, interference power and bandwidth spreading. The effect of the various parameters on the receiver's performance was analyzed and discussed.

From the general representation of the narrowband nonstationary random process, other forms of nonstationary interference can be proposed and their effect on communication receivers can be derived by similar approaches. Although the derived performance of the spread spectrm receiver was developed for BPSK signal modulation with direct sequence bandwidth spreading, the general results can be modified and extended to obtain performance evaluations of receivers in which other modulation schemes are employed.

II. NONSTATIONARY RANDOM PROCESSES

A. NONSTATIONARY NARROWBAND RANDOM PROCESSES

A random process is said to be narrowband if its power spectral density is zero except for a narrow frequency region (W Hz) around a high carrier frequency (f_o), that is,

$$W << 2\pi f_o \quad \text{and} \quad 2\pi f_o >> 1$$

If $X(t)$ is a sample function of such a real random process with zero mean, it may be expressed as: [Ref. 4]

$$X(t) = X_c(t)\cos 2\pi f_o t - X_s(t)\sin 2\pi f_o t \tag{2.1}$$

where the power spectral density of the random processes $X_c(t)$ and $X_s(t)$ is zero except for a narrow frequency region (W Hz) around $f = 0$. The random processes $X_c(t)$ and $X_s(t)$ are referred to as the quadrature components of $X(t)$.

Random processes can be generally classified into stationary and nonstationary processes. If the joint probability density function (p.d.f.) of a process $X(t)$ taken at arbitrary times $t_1, t_2 \ldots t_n$ is invariant to arbitrary time shifts for any integer n, such a stochastic process is said to be stationary [Ref. 5]. A random process is nonstationary if it does not have the above properties. A weaker form of stationarity is the so-called wide sense stationarity (W.S.S.) involving first and second order moments of a random process [Ref. 6]. The representation of Eq. 2.1 normally implies a W.S.S. random process $X(t)$.

We propose here to represent a nonstationary narrowband random process in a form analogous to that of Eq. 2.1 and to study the statistics of the associated quadrature components. This is accomplished by analyzing the output of a

narrowband filter when the input is an arbitrary nonstationary process. Before attempting this, a convenient method of specifying a narrowband filter is developed first.

1. Lowpass Equivalent of a Narrowband Filter

Any bandpass filter can be specified in terms of low-pass filter equivalents. Let $h_L(t)$ be the impulse response of a low-pass filter and $H_L(f)$ be the Fourier Transform of $h_L(t)$, that is,

$$h_L(t) \overset{F}{\Longleftrightarrow} H_L(f) = A(f)e^{j\theta(f)} \tag{2.2}$$

where $H_L(f)$ is not necessarily symmetric about $f = 0$ so that $h_L(t)$ is not necessarily real. Then the Fourier Transform $H_B(f)$ of a bandpass filter having impulse response $h_B(t)$ can be specified as follows: [Ref. 7]

$$h_B(t) \overset{F}{\Longleftrightarrow} H_B(f) = H_L(f - f_o) + H_L(-(f + f_o)) \tag{2.3}$$

As shown in Figure 2.1, $H_B(f)$ is realized by summing the frequency up shifted (by f_o) and the frequency reversed and down shifted (by f_o) Fourier Transform of the low-pass filter. The negative sign in the term $H_L(-(f + f_o))$ is due to the frequency reversion of $H_L(f)$ described above.

We can remark that in general $h_L(t)$ is a complex quantity. However, since the focus is on generating real narrowband random processes, we will require that $h_B(t)$ is a real function of t. By inverse Fourier Transformation of Eq. 2.3 and by expressing $h_L(t)$ in the following complex form,

$$h_L(t) = h_{Lr}(t) + jh_{Li}(t) \tag{2.4}$$

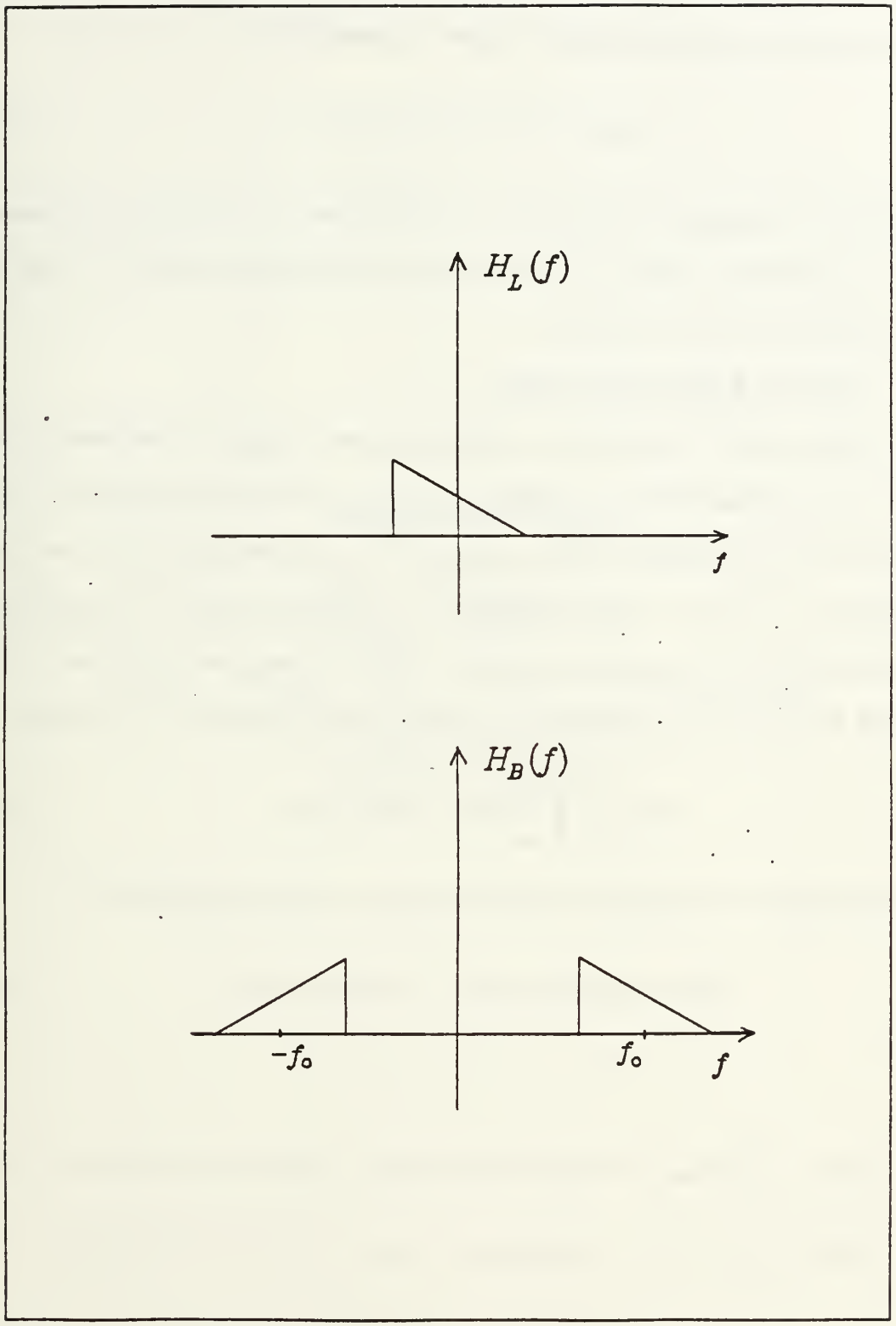

Figure 2.1 Graphic Representation of $H_L(f)$ and $H_B(f)$

where both $h_{Lr}(t)$ and $h_{Li}(t)$ are real functions of t, we can obtain the impulse response $h_B(t)$ of a narrowband filter as [see Appendix A]

$$h_B(t) = 2Re\left\{h_L(t)e^{j2\pi f_o t}\right\} \tag{2.5}$$

where $Re\{(\cdot)\}$ represents the real part of the function in brackets. It is demonstrated in Appendix A that $h_{Lr}(t)$ must be an even function and $h_{Li}(t)$ must be an odd function if $h_b(t)$ is to be real.

2. Output of a Narrowband Filter

In the case of a stationary random process input, the statistics of the output of a narrowband filter is well-known [Ref. 4]. We will investigate the more general case where the input random process to a narrowband filter is real but nonstationary. Let $Y(t)$ be the output due to a real input signal $X(t)$ applied to a narrowband filter having transfer function $H_B(f)$ as described in Section 1 [Fig. 2.2]. Then $Y(t)$ can be expressed as the convolution of $X(t)$ and $h_B(t)$ namely

$$Y(t) = \int_{-\infty}^{\infty} h_B(t-\alpha)X(\alpha)d\alpha \tag{2.6}$$

It is demonstrated in Appendix B that $Y(t)$ can be further expressed as

$$Y(t) = 2X_c(t)\cos 2\pi f_o t - 2X_s(t)\sin 2\pi f_o t \tag{2.7}$$

where

$$X_c(t) = \int_{-\infty}^{\infty} \left[h_{Lr}(t-\alpha)\cos 2\pi f_o\alpha + h_{Li}(t-\alpha)\sin 2\pi f_o\alpha\right] X(\alpha)d\alpha \tag{2.8}$$

$$X_s(t) = \int_{-\infty}^{\infty} \left[h_{Li}(t-\alpha)\cos 2\pi f_o\alpha - h_{Lr}(t-\alpha)\sin 2\pi f_o\alpha\right] X(\alpha)d\alpha \tag{2.9}$$

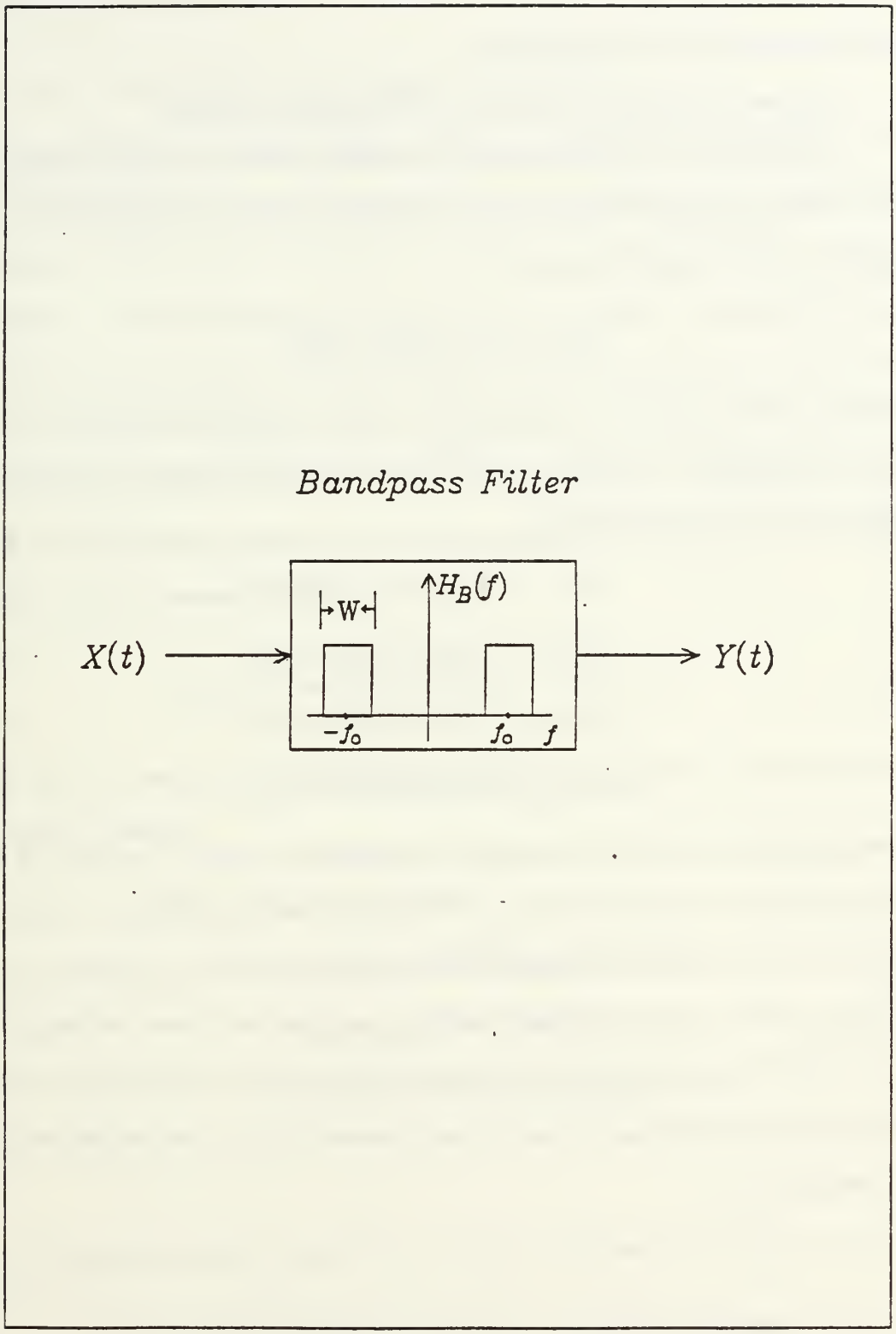

Figure 2.2 Narrowband Filtering of Real Input X(t)

There is a certain degree of similarity in the mathematical form of Eq. 2.7 and Eq. 2.1. However, the properties of $X_c(t)$ and $X_s(t)$ given by Eq. 2.8 and Eq. 2.9 respectively must now be established.

3. Output Correlation Function for Nonstationary Input

By definition, the autocorrelation function $Ry(t_1, t_2)$ of any random process $Y(t)$ is the expected value of the product of $Y(t_1)$ and $Y(t_2)$ for arbitrary time instants t_1 and t_2 [Ref. 5], that is

$$R_y(t_1, t_2) = E\{y(t_1)y(t_2)\} \tag{2.10}$$

In order to obtain $R_y(t_1, t_2)$ for the output $Y(t)$ of the filter described in Section 2, it will be necessary to evaluate the following quantities (since $Y(t)$ is the linear combination of $X_c(t)$ and $X_s(t)$)

$$R_c(t_1, t_2) \triangleq E\{X_c(t_1)X_c(t_2)\} \tag{2.11}$$

$$R_s(t_1, t_2) \triangleq E\{X_s(t_1)X_s(t_2)\} \tag{2.12}$$

$$R_{cs}(t_1, t_2) \triangleq E\{X_c(t_1)X_s(t_2)\} \tag{2.13}$$

$$R_{sc}(t_1, t_2) \triangleq E\{X_s(t_1)X_c(t_2)\} \tag{2.14}$$

The four quantities above are complicated functions of t_1 and t_2 [See App. B]. It can be observed that in general $R_c(t_1, t_2) \neq R_s(t_1, t_2)$ and $R_{cs}(t_1, t_2) \neq -R_{sc}(t_1, t_2)$; unlike the case of stationary narrowband process, both the quadrature components have identical autocorrelation function and the two cross-correlation functions are null if both $X_c(t)$ and $X_s(t)$ are real [Ref. 4]. The autocorrelation function $R_y(t_1, t_2)$ of the nonstationary narrowband process $Y(t)$ can be formulated as follows [See App. B]:

$$\begin{aligned} R_y(t_1, t_2) = 4\Big[& R_c(t_1, t_2)\cos 2\pi f_o t_1 \cos 2\pi f_o t_2 + R_s(t_1, t_2)\sin 2\pi f_o t \sin \pi f_o t_2 \\ & - R_{cs}(t_1, t_2)\cos 2\pi f_o t_1 \sin 2\pi f_o t_2 - R_{sc}(t_1, t_2)\sin 2\pi f_o t \cos 2\pi f_o t_2 \Big] \end{aligned} \tag{2.15}$$

It is clear that $Ry(t_1, t_2)$ is also a linear combination of $R_c(t_1, t_2), R_s(t_1, t_2), R_{cs}(t_1, t_2)$ and $R_{sc}(t_1, t_2)$.

B. A MODEL FOR THE NONSTATIONARY INPUT

The results of the previous sections will be applied now to a specific general class of nonstationary random processes which are generated by a system to be described now. This is done in order to continue the development for a class of nonstationary random processes of interest and to be able to apply the results to some practical problems involving jamming of spread spectrum communication systems. Let the nonstationary input $X(t)$ described previously be the result of mixing a stationary random process $W(t)$ with a deterministic signal $q(t)$ as shown in Fig. 2.3. We further assume that the autocorrelation function $R_w(t_1, t_2)$ of the stationary random process $W(t)$ is

$$R_w(t_1, t_2) = E[W(t_1)W(t_2)] = \delta(t_2 - t_1) \tag{2.16}$$

That is, $W(t)$ is assumed to be a white process with unit power spectral density (PSD) level. Therefore

$$\begin{aligned} R_x(t_1, t_2) &= E[X(t_1)X(t_2)] \\ &= E[W(t_1)q(t_1)W(t_2)q(t_2)] \\ &= q(t_1)q(t_2)E[W(t_1)W(t_2)] \\ &= q^2(t_1)\delta(t_2 - t_1) = q^2(t_2)\delta(t_2 - t_1) \end{aligned} \tag{2.17}$$

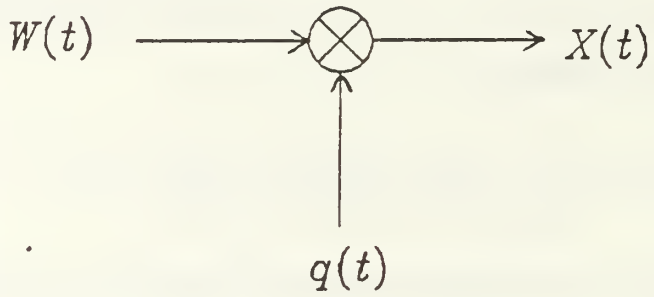

Figure 2.3 Nonstationary Input X(t)

since $R_x(t_1, t_2)$ is zero unless $t_2 = t_1$. We can now apply the results from Appendix B in order to characterize the output of a narrowband filter when its input is a nonstationary random process of the type being described in this section. It is demonstrated in Appendix C that the autocorrelation terms of Equations 2.11 - 2.14 simplify significantly when $X(t) = q(t)W(t)$, namely

$$R_c(t_1, t_2) = R_s(t_1, t_2) \tag{2.18}$$

and

$$R_{cs}(t_1, t_2) = R_{sc}(t_1, t_2) = 0 \tag{2.19}$$

Finally, the autocorrelation function $R_y(t_1, t_2)$ for the nonstationary process $Y(t)$, namely the output of the narrowband filter, has the following form: [see App. C]

$$R_y(t_1, t_2) = 2\cos 2\pi f_o(t_2 - t_1) \int_{-\infty}^{\infty} h_L(t_1 - \alpha) h_L(t_2 - \alpha) q_s(\alpha) d\alpha \tag{2.20}$$

where

$$q_s(t) = q^2(t) \tag{2.21}$$

Observe that $R_y(t_1, t_2)$ is not a function of the time difference $(t_2 - t_1)$, so that $Y(t)$ is (as expected) a nonstationary random process.

C. A SPECIFIC EXAMPLE

In the previous sections, we have established a representation in general form for a narrowband nonstationary random process generated by applying the mixture process $q(t)W(t)$ at the input of a narrowband filter. As a specific example, it is now desired to use these results to model and characterize a pulsed noise jammer that is processed by a narrowband filter. Assuming that we have a bi-level pulsed noise jammer, we can model the jamming signal $X(t)$ as the result of mixing white noise

$W(t)$ of unit PSD level with a bi-level deterministic periodic signal $q(t)$. Such a jamming signal present in the communication channel would cause a typical receiver to produce a jamming component at the output of the receiving front end narrowband filter. This component is denoted $Y(t)$ as shown in Figure 2.4.

The autocorrelation function $R_x(t_1, t_2)$ of the input process to the narrowband filter is given by Eq. 2.17 while the corresponding output autocorrelation $R_y(t_1, t_2)$ is given by Eq. 2.20. T_q is the period of the periodic signal $q(t)$ which remains at the level A for the time interval $[o, \rho T_q]$ and at the low level C for the time interval $[\rho T_q, T_q], 0 < \rho < 1$. [Fig. 2.5] The narrowband filter $H_B(t)$ is based on a low-pass equivalent which is assumed to have impulse response $h_L(t) = B \cdot e^{-Bt}U(t)$ where $U(t)$ is the unit step function, and B specifies the 3db point of the filter. The details of the derivation are presented in Appendix D, where it is demonstrated that for the special case under consideration, Eq. 2.20 becomes

$$R_y(t_1, t_2) = 2\cos 2\pi f_o(t_2 - t_1)\left\{\frac{A^2 B}{2} e^{-B(t_1+t_2)} e^{2B\,\mathrm{Min}(t_1,t_2)} - \right.$$
$$\frac{B(A^2 - C^2)}{2} e^{-B(t_1+t_2)}\left[e^{2B\,\mathrm{Min}(t_1,t_2)}([r] - [s]\right. \qquad (2.22)$$
$$\left.\left. + \frac{e^{2BT_q} \cdot e^{2BT_q[s]} - e^{2B\rho T_q} \cdot e^{2BT_q[r]}}{1 - e^{-2BT_q}}\right]\right\}$$

where $[z]$ is the largest integer less than or equal to z

$$r = -\rho + \frac{1}{T_q}\mathrm{Min}(t_1, t_2), \qquad (2.23)$$

$$s = -1 + \frac{1}{T_q}\mathrm{Min}(t_1, t_2) \qquad (2.24)$$

and

$$\mathrm{Min}(t_1, t_2) = \text{ minimum of } t_1 \text{ and } t_2$$

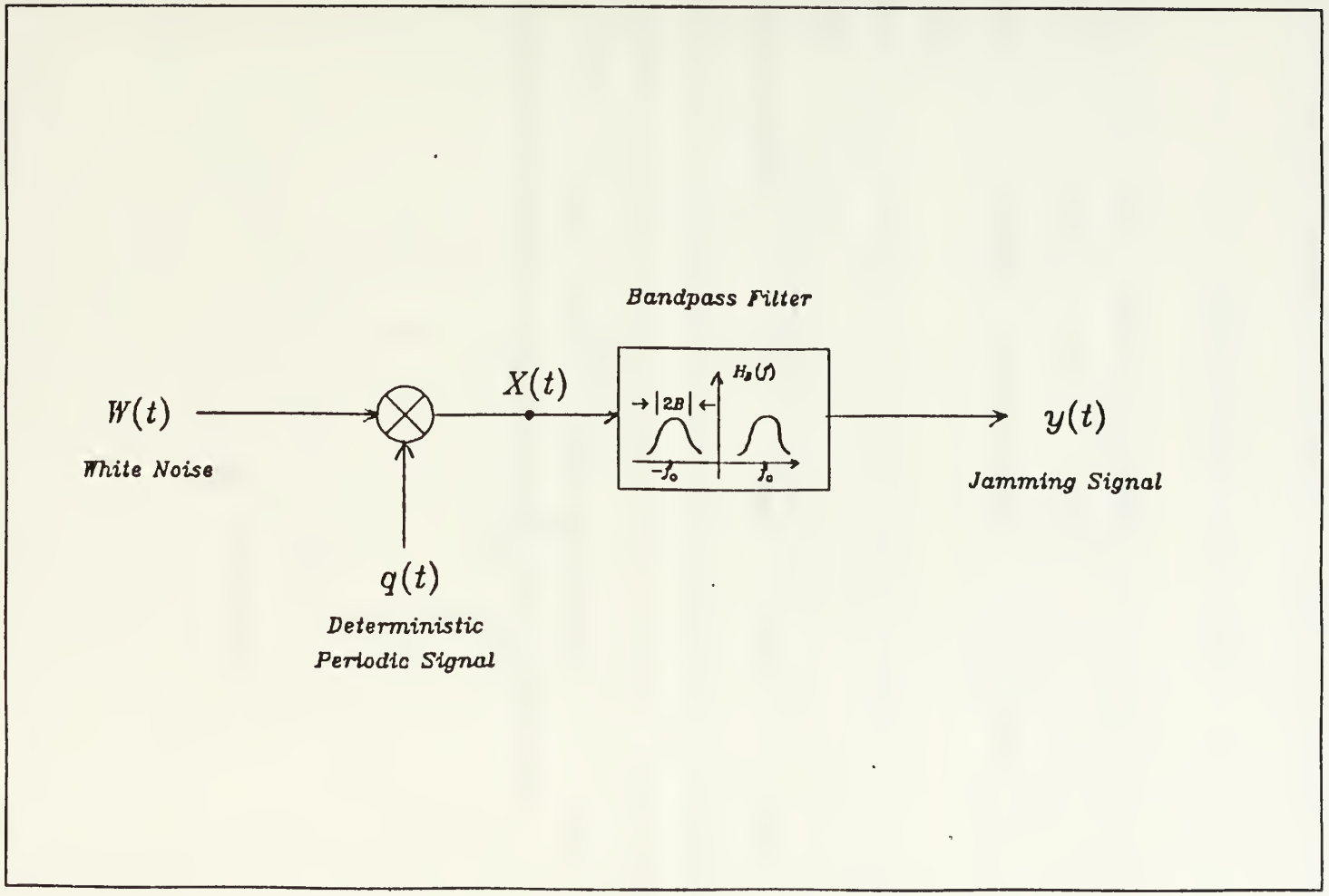

Figure 2.4 Schematic Representation of the Bi-level Jammer Model

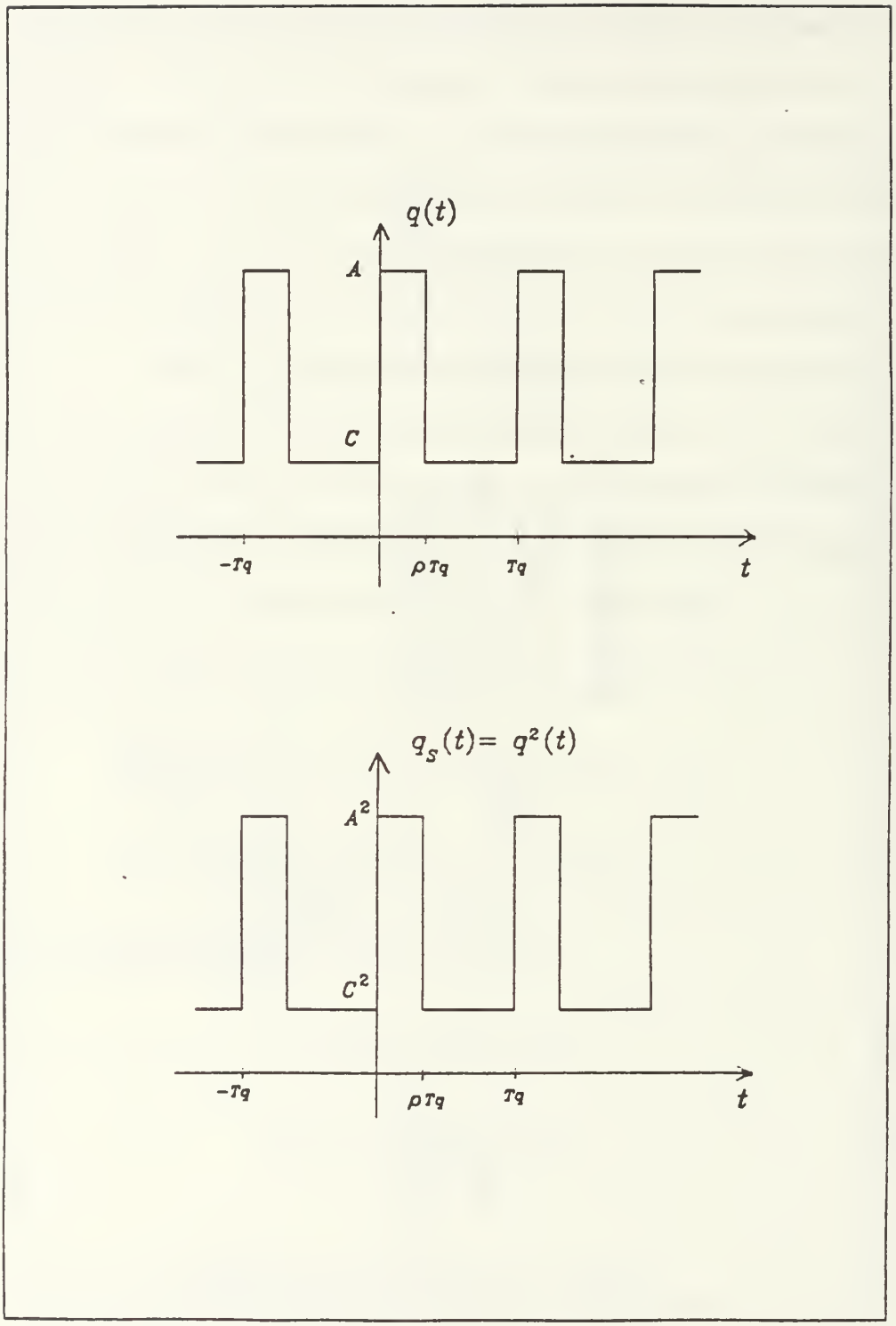

Figure 2.5 Functions q(t) and $q_s(t)$

Although equation 2.22 is not a simple mathematical form, it is possible to derive the average power of the random process $Y(t)$, by time averaging $R_y(t,t)$. The details are again presented in Appendix D, where it is demonstrated that

$$\overline{R_y(t,t)} = B[A^2\rho + c^2(1-\rho)] \tag{2.25}$$

This result can be easily verified from the assumptions made at the beginning of this paragraph. Furthermore, it can be seen that for the special case under consideration, $\overline{R_y(t,t)}$ represents the jammer power at the output of the narrowband filter $H_B(f)$.

It has thus been shown that a nonstationary narrowband process can be represented by the nonstationary quadrature components in a form analogous to that for the representation of wide sense stationary narrowband processes. A general expression of the correlation function for a filtered nonstationary input is obtained. The results are applied to a special case in order to model a bi-level pulsed noise jammer. The effects on a spread spectrum communication receiver due to such a pulsed noise jamming signal will be investigated in the next chapter.

III. EFFECT OF SPREAD SPECTRUM SYSTEM ON NONSTATIONARY NOISE

A. MODEL FOR THE SPREAD SPECTRUM RECEIVER

In spread spectrum modulation, digital information is transmitted by employing a trasmission bandwidth which is much larger than the minimum bandwidth required to transmit the digital information via conventional means. In the spread spectrum receiver, the demodulation must be accomplished, in part, by correlation of the received signal with a replica of the "spreading" signal used in the transmitter in order to recover the digital information signal. If the bandwidth is spread by direct modulation of a data-modulated carrier with a wideband spreading signal or code, the technique is referred to as direct sequence (abbreviated DS) spread spectrum modulation.

The simplest form of DS spread spectrum modulation is DS-BPSK spread spectrum transmission where a binary phase shift keyed (BPSK) modulated carrier is spread by a wideband "code signal." [Ref. 2]. The spreading operation can be mathematically represented as a multiplication of the carrier by a function $c(t)$ which takes on the values ± 1 at a digital rate R_c periodically. (Fig. 3.1) The transmitted spread spectrum signal is received together with some type of interference and/or Gaussian noise. Demodulation is accomplished in part by remodulating with the spreading code $c(t)$. The process is commonly referred to as despreading and is a critical function in all spread spectrum systems.

A simplified model of the DS-BPSK receiver is illustrated in Fig. 3.2. The figure shows the received signal $r(t)$ first processed through a front-end bandpass

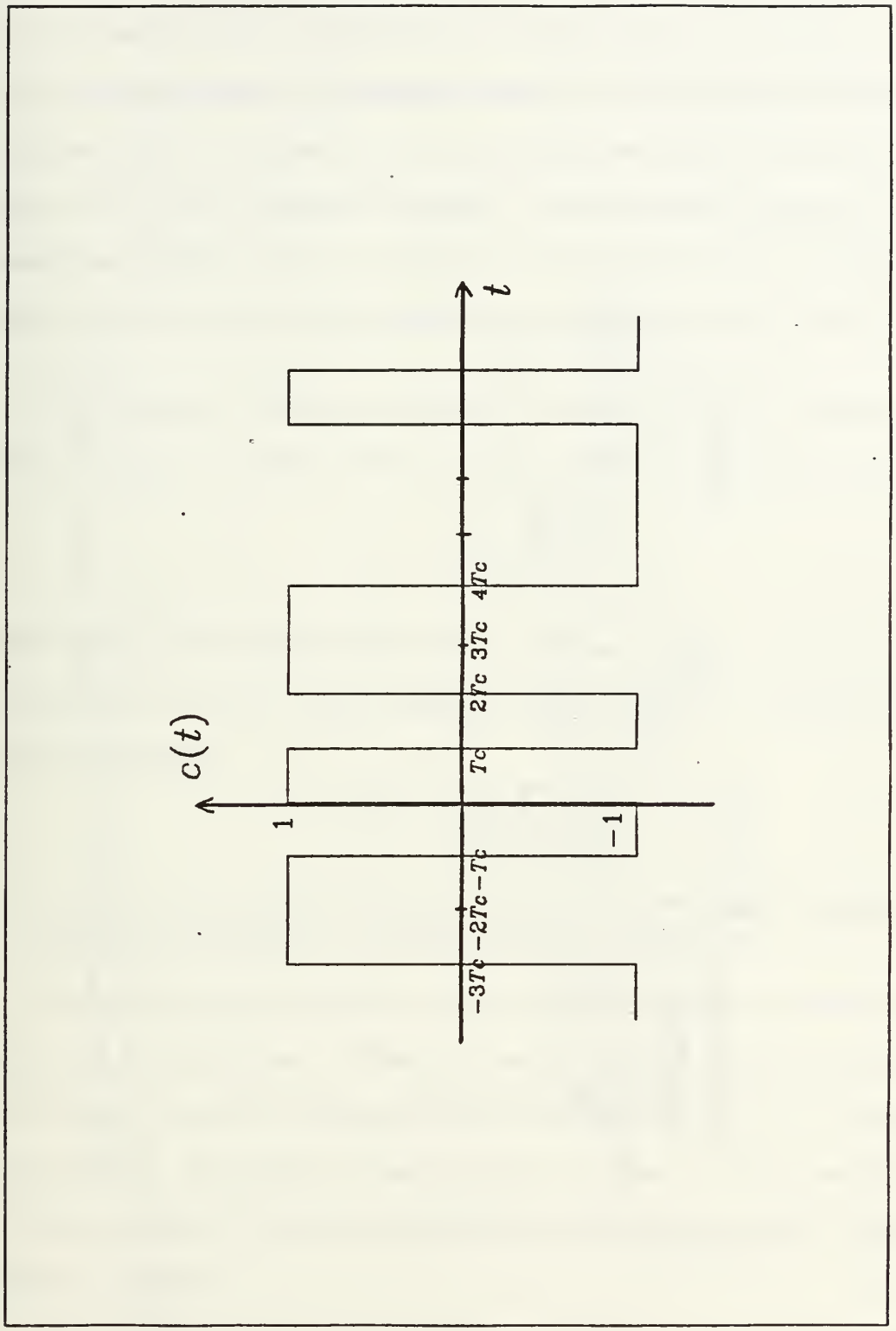

Figure 3.1 BPSK Spreading Code c(t)

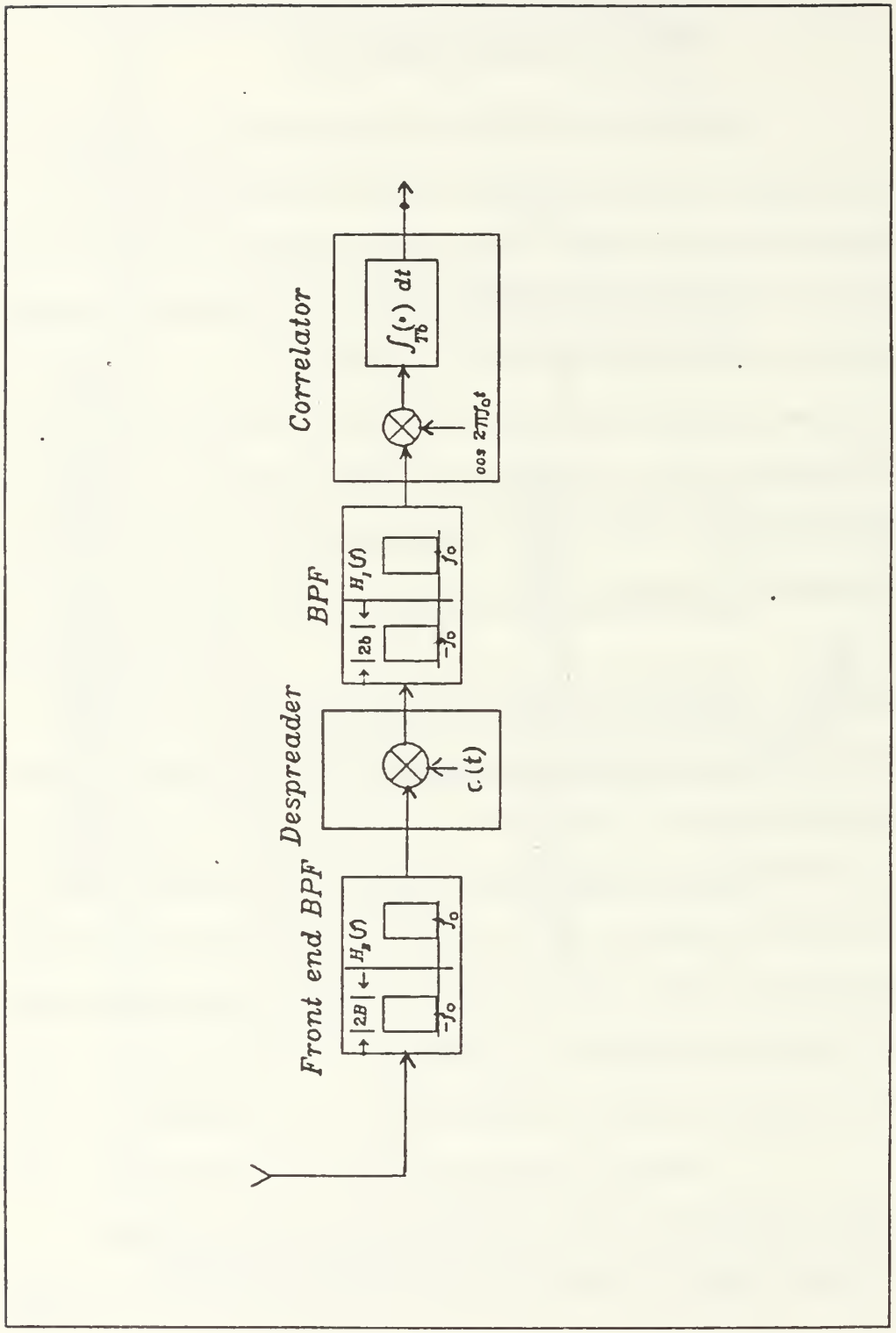

Figure 3.2 Simplified DS-BPSK Spread Spectrum Receiver

filter centered at the carrier frequency f_0 and having a bandwidth wide enough for the spreading signal (contaminated by thermal noise and perhaps a jammer) to be allowed through with negligible distortion. The output of the front-end bandpass filter is then mixed with a local synchronized replica of the code spreading signal $c(t)$ in order to despread the signal. The despreading operation produces a contaminated BPSK signal from which the digital information can be recovered by conventional techniques using a filter and a correlator as shown in Fig. 3.2.

It is well-known that in the absence of any jamming, the perfomance of the receiver in Fig. 3.2 in terms of the bit error probability (P_b) is given by: [Ref. 2]

$$P_b = Q\left(\sqrt{\frac{2E_b}{N_o}}\right) \tag{3.1}$$

where R_b is the bit energy of the received signal, N_o is the one-sided power spectral density level of the AWGN interference and $Q(\cdot)$ is the complementary error function defined by

$$Q(x) = \frac{1}{\sqrt{2\pi}} \int_x^\infty e^{-\frac{t^2}{2}} dt \tag{3.2}$$

B. EFFECT OF NONSTATIONARY NOISE ON THE DESPREADER AND BIT DETECTOR ON NONSTATIONARY NOISE

The jamming signal produced by the bi-level pulsed noise jammer may not necessarily be narrowband. However, after the filtering operation performed by the receiver's front-end bandpass filter the jamming signal can be considered to be narrowband. We therefore investigate here the effect of the despreader and the bit detector system on the input nonstationary narrowband random signal which models the jammer.

The receiver of Figure 3.2 is now assumed to have a narrowband nonstationary zero mean input $y(t)$ as illustrated in Figure 3.3. The output of the bandpass filter

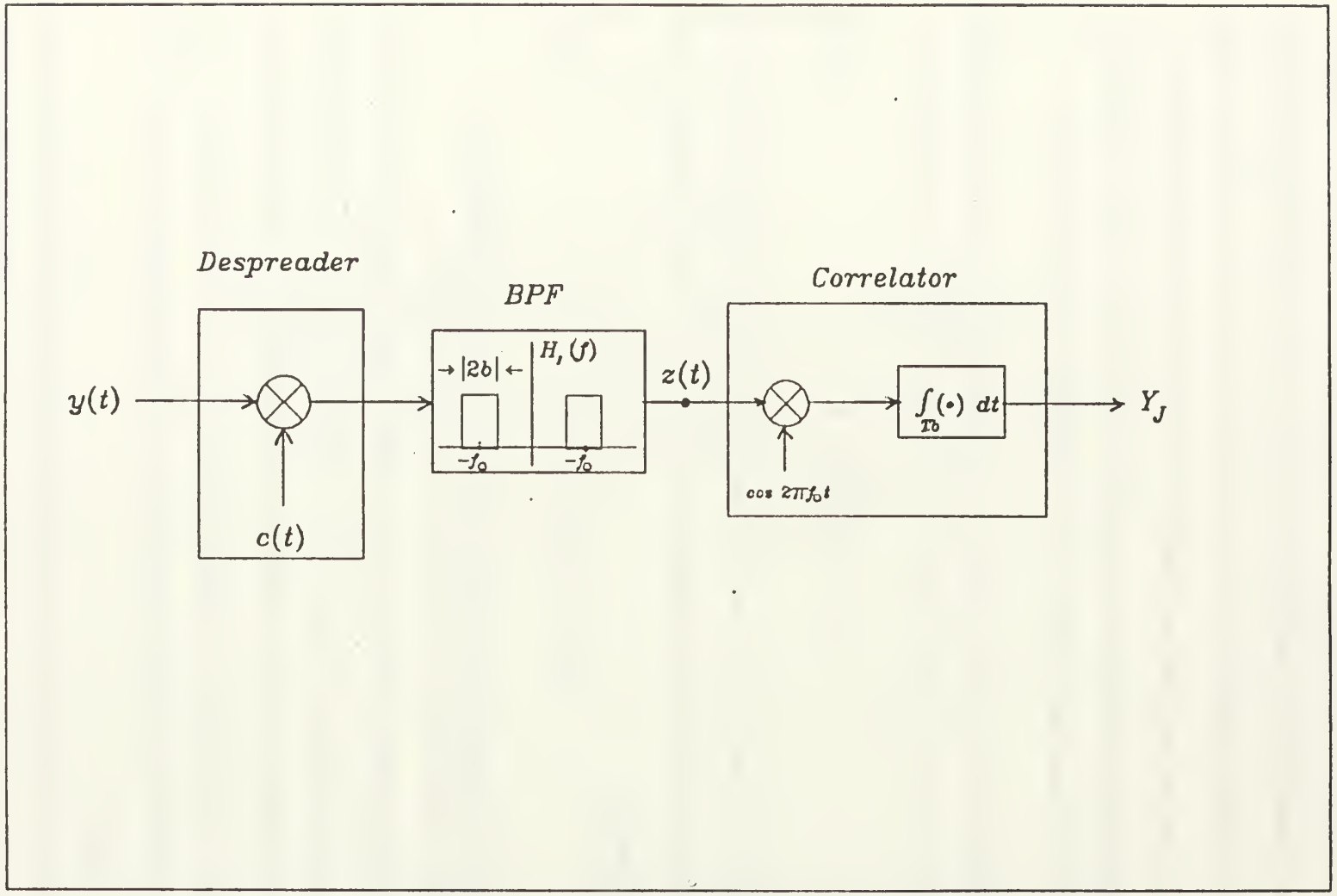

Figure 3.3 Simplified DS–BPSK Spread Spectrum Receiver for Nonstationary Narrowband Input

is denoted by $z(t)$ while the bandpass filter impulse response is denoted $h_I(t)$ and can be specified in terms of a low-pass filter equivalents denoted $h_I(t)$. The output of the receiver due to the input $y(t)$ is denoted Y_y. It can be seen that

$$z(t) = y(t)c(t) * h_I(t) = \int_{-\infty}^{\infty} h_I(t-\tau)y(\tau)c(\tau)d\tau \tag{3.3}$$

and

$$Y_J = \int_0^{T_b} z(t)\cos 2\pi f_0 t dt$$

which can also be expressed as

$$Y_J = \int_0^{T_b} \left[\int_{-\infty}^{\infty} h_I(t-\tau)y(\tau)c(\tau)d\tau \right] dt \tag{3.4}$$

The jamming of the transmitted signal is always being considered as an action of adding a nonstationary Gaussian random process to the signal. As will be seen in the analysis to be carried out in Chapter IV, part B, the effect of the jammer on the receiver's performance is completely accounted for by evaluating the variance of the output of the bit detector. That is, only the variance of Y_J will be established and the other statistical properties of Y_J which have no direct influence on the systems bit-error probability will be neglected.

The variance σ_J^2 can be shown to be given by an infinite sum of terms, namely

$$\sigma_J^2 = \sum_{n=-\infty}^{\infty} C_n \int_{-\infty}^{\infty} H_i(f)H_I(nR_q - f)P_c(-f)P_c(f - nR_q)\cdot$$

$$\int_{-\infty}^{\infty} H_L(u)H_L(nR_q - u)\left[S_c(f + f_0 - u) + S_c(f - f_0 - u)\right] dudf \tag{3.5}$$

where R_q is the period of the nonstationary jamming signal and C_n is given by:

$$C_n = \begin{cases} A^2\rho + c^2(1-\rho) & ; n = 0 \\ \rho(A^2 - C^2)\dfrac{\sin n\pi\rho}{n\pi\rho}e^{jn\pi\rho} & ; n \neq 0 \end{cases}$$

It can be seen from Eq. 3.5 that σ_J^2 is a function of the duration T_b of the information bit, the duration T_c of the spreading code, chips, and T_q, the jammer pulsing period. However, practical spread spectrum systems utilize spreading codes for which the chip duration is very much smaller than the information data bit duration [Ref. 8]. That is

$$T_c << T_b \qquad \text{or} \qquad R_c >> R_b$$

where R_c is just T_c^{-1}, the chip rate, and R_b is T_b^{-1}, the bit rate. It is therefore possible to define here two classes of jammers, namely fast jammers for which the pulse repetition period T_q is of the same order of magnitude as T_c, so that the jammer pulsing rate is much larger than the data rate, and slow jammers for which T_c is of the same order of magnitude as T_b. The effect of the jammer pulsing rate on the variance σ_J^2 will be examined separately for both cases.

1. Variance σ_J^2 for the Fast Jammer

Consider first the Fourier Transform $P_c(f)$ of the function $P_c(f)$ defined in Eq. E-2, namely

$$P_c(f) = \int_0^{T_b} \cos 2\pi f_0 t e^{-j2\pi ft} dt = G(f - f_0) + G(f + f_0) \tag{3.6}$$

where

$$G(f) = \frac{T_b}{2} \text{ sinc } (fT_b) e^{-j2\pi fT_b}$$

We can see that $P_c(f)$ is significant for $f = \pm f_0$ over a restricted frequency band. Similarly, $P_c((f - nR_q)$ is significant for $f = \pm(f_0 + nR_q)$ over a similarly restricted frequency band. The functions $P_c(f)$ and $P_c(f - nR_q)$ are diagramed in Figure 3.4 from which it is possible to observe that if

$$f_0 - nR_q + R_b \quad << \quad f_0 - R_b$$

or equivalently, if

$$2R_b \quad << \quad nR_q \tag{3.7}$$

essentially no spectral overlap of the frequency functions occur. This condition except for $n = 0$ is satisfied for what has been defined as a fast jammer since $R_q >> R_b$ under fast jamming.

It is possible to conclude therefore that in the case of a fast pulsed jamming environment, the only contribution due to the infinite sum of terms that make up the variance σ_J^2 is the term $n = 0$ (See Eq. 3.5). Therefore

$$\begin{aligned}\sigma_J^2 \; &= C_0 \int_{-\infty}^{\infty} H_I(f) H_I(-f) P_c(-f) \\ &\int_{-\infty}^{\infty} H_L(u) H_L(-u) \left[S_c(f + f_0 - u) + S_c(f - f_0 - u) \right] du df\end{aligned} \tag{3.8}$$

and substituting in Eq. 3.8 the corresponding mathematical description of the functions $H_I(\cdot), H_L(\cdot), P_c(\cdot)$ and $S_c(\cdot)$ as given in Eqs. E.3, G.6, G.8 and G.17, results in

$$\begin{aligned}\sigma_J^2 \; = \frac{C_0 T_b}{8} \Bigg\{ & 1 + \left(\frac{2}{B^2 T_b T_c} - \frac{1}{B T_c} \right) \left(1 - e^{-B T_c} \right) - \frac{1 + e^{-B T_c}}{B T_b} \\ & + \left(2e^{-b T_b} - 1 \right) \left[\frac{B^2}{b T_b (B^2 - b^2)} - \frac{B(B^2 + b^2)}{b T_b T_c (B^2 - b^2)^2} + \right. \\ & \left. \frac{B e^{-B T_c} e^{-b T_c}}{2 b T_b T_c (B + b)^2} + \frac{B e^{-B T_c} e^{b T_c}}{2 b T_b T_c (B - b)^2} \right] \Bigg\}\end{aligned} \tag{3.9}$$

The details of the derivation of this result are presented in Appendix G.

2. Variance σ_J^2 for the Slow Jammer

In the case of a slow pulsed jamming environment, the condition $R_q >> R_b$ is not satisfied, therefore a certain degree of overlapping between the spectral factors that make up the expression for σ_J^2 will occur. While the infinite sum of

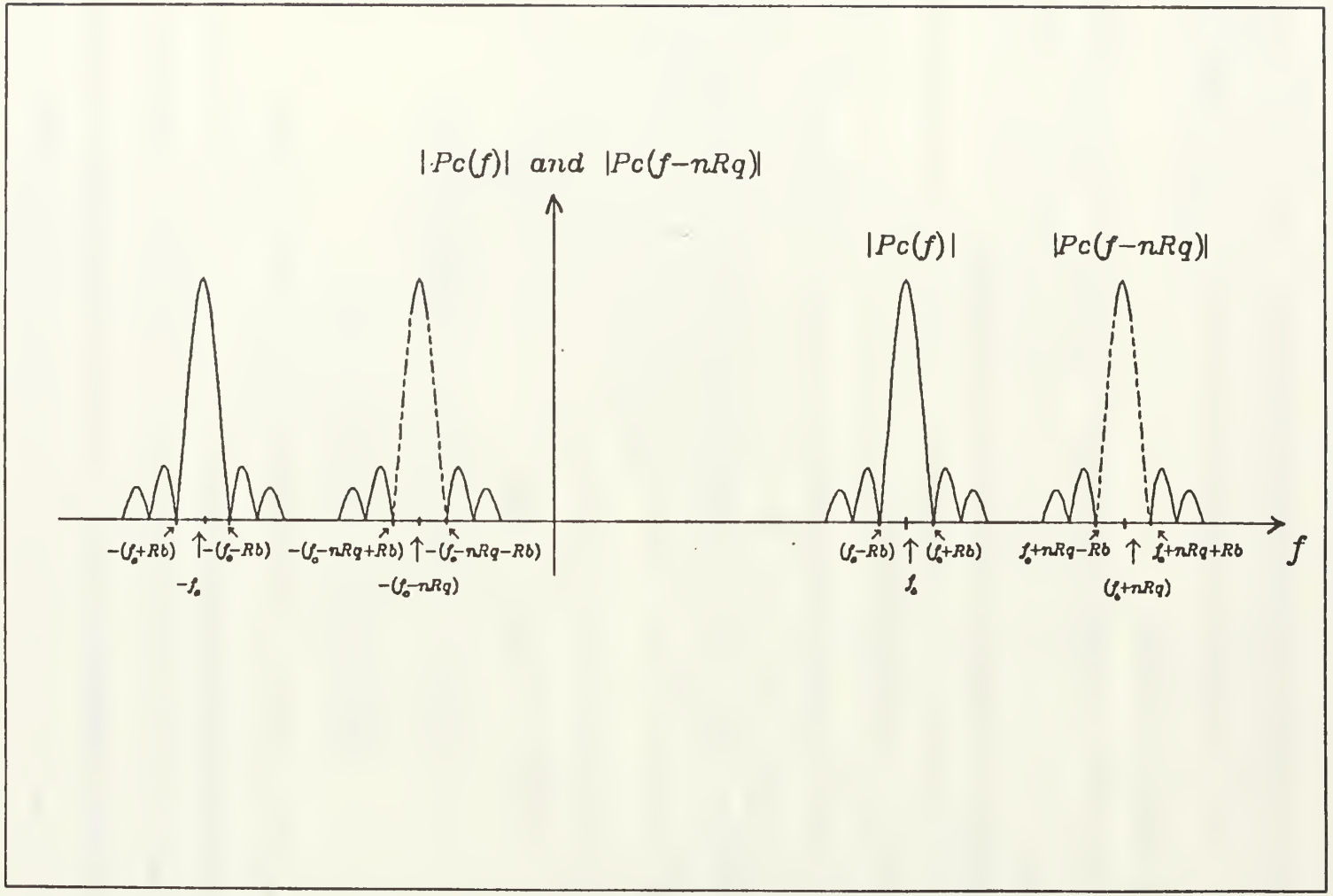

Figure 3.4 Functions Pc(f) and Pc(f−nRq)

Eq. 3.5 can be approximated accurately by a finite sum, the number n_0, of terms needed in the approximation will be such that

$$n_0 R_q >> 2R_b$$

or equivalently

$$n_0 >> \frac{2R_b}{R_q} \tag{3.10}$$

In this case, the result for σ_J^2 becomes

$$\sigma_J^2 = \sum_{k=-n_0}^{n_0} C_k \int_{-\infty}^{\infty} H_I(f) H_I(kR_q - f) P_c(-f) P_c(f - kR_q)$$
$$\int_{-\infty}^{\infty} H_L(u) H_L(kR_q - u) \left[S_c(f + f_0 - u) + S_c(f - f_0 - u)\right] du df \tag{3.11}$$

It is also clear that as k increases, $|C_k|$ decreases so that the sum involved can perhaps be further truncated. The computation of σ_J^2 in this case becomes quite complicated, however using numerical integration, σ_J^2 can be obtained quite accurately.

IV. PERFORMANCE OF THE SPREAD SPECTRUM COMMUNICATION SYSTEM

A. GENERAL OUTLINE

In Chapter III, a complete derivation for σ_J^2, the variance of the Gaussian random variable that quantifies the power contribution of a bi-level, nonstationary narrowband jamming signal at the output of a DS-BPSK Spread Spectrum Modulation receiver, has been undertaken. A diagram of the spread spectrum receiver is shown in Fig. 3.1. The receiver structure is optimized based on principles of Maximum A Posteriori (MAP) detection for binary modulation schemes. The received signal and noise is first processed by the front-end bandpass filter which has a bandwidth just wide enough to pass the spread signal and the in-band noise. The narrowband signal is then processed by the despreader which consists of a multiplier mixing the received signal with a synchronozed local replica of the spreading code signal. A second bandpass filter having a bandwidth proportional to the information bandwidth follows the despreader, so as to further eliminate the noise power being presented to the remainder of the receiver. The data signal is then demodulated by a correlator and finally, a decision is produced every T_b seconds which is translated into 0 or 1 data bits. This generates a MAP estimate of the digital data at the output of the receiver.

The performance of such a receiver is usually characterized by the probability of error, which is, in essence, the probability of an incorrect decision made at the receiver. The probability of error can be further categorized into symbol error and bit error probability. However, for the case of Binary Phase Shift Keyed (BPSK)

modulation, the two error probabilities are equivalent and provide the basis for specifying the receiver's performance.

In the next section, we investigate the performance for the case in which a BPSK modulated signal is spread by direct sequence methods, and the signal is received in AWGN interference as well as the bi-level pulsed noise jammer described and analyzed in previous chapters.

B. RECEIVER PERFORMANCE FOR BPSK MODULATION

The structure of a spread spectrum correlation reciever is shown once again in Fig. 4.1. In BPSK modulation, the two transmitted signals are [Ref. 4]

$$\begin{aligned} s_1(t) &= \sqrt{\frac{2E_b}{T_b}}\cos 2\pi f_o t \qquad 0 \le t \le T_b \quad \text{and} \\ s_2(t) &= -\sqrt{\frac{2E_b}{T_b}}\cos 2\pi f_o t \qquad 0 \le t \le T_b \end{aligned} \tag{4.1}$$

where E_b is the energy of each signal and T_b is the duration of each signal. Since each signal represents a single information bit, E_b is the energy per bit and T_b^{-1} is the bit rate.

At the output of the second bandpass filter, the signal $y(t)$ can be regarded as the summation of the transmitted signal $s_i(t)$, narrowband noise $N_{th}(t)$, and the jamming signal $y_J(t)$ convolved with the impulse response $h_I(t)$ of the bandpass filter. That is,

$$\begin{aligned} y(t) &= \Big[s_i(t) + N_{th}(t) + y_J(t)c(t)\Big] * h_I(t) \\ & \quad i = 1 \text{ or } 2 \end{aligned} \tag{4.2}$$

Hence,

$$\begin{aligned} Y &\triangleq \int_0^{T_b} y(t)\cos 2\pi f_o t dt \\ &= \int_0^{T_b} S_i(t) * h_I(t)\cos 2\pi f_o t dt + \int_0^{T_b} N_{th}(t)C(t) * h_I(t)\cos 2\pi f_o t dt \\ &+ \int_0^{T_b} y_J(t)c(t) * h_I(t)\cos 2\pi f_o t dt \end{aligned} \tag{4.3}$$

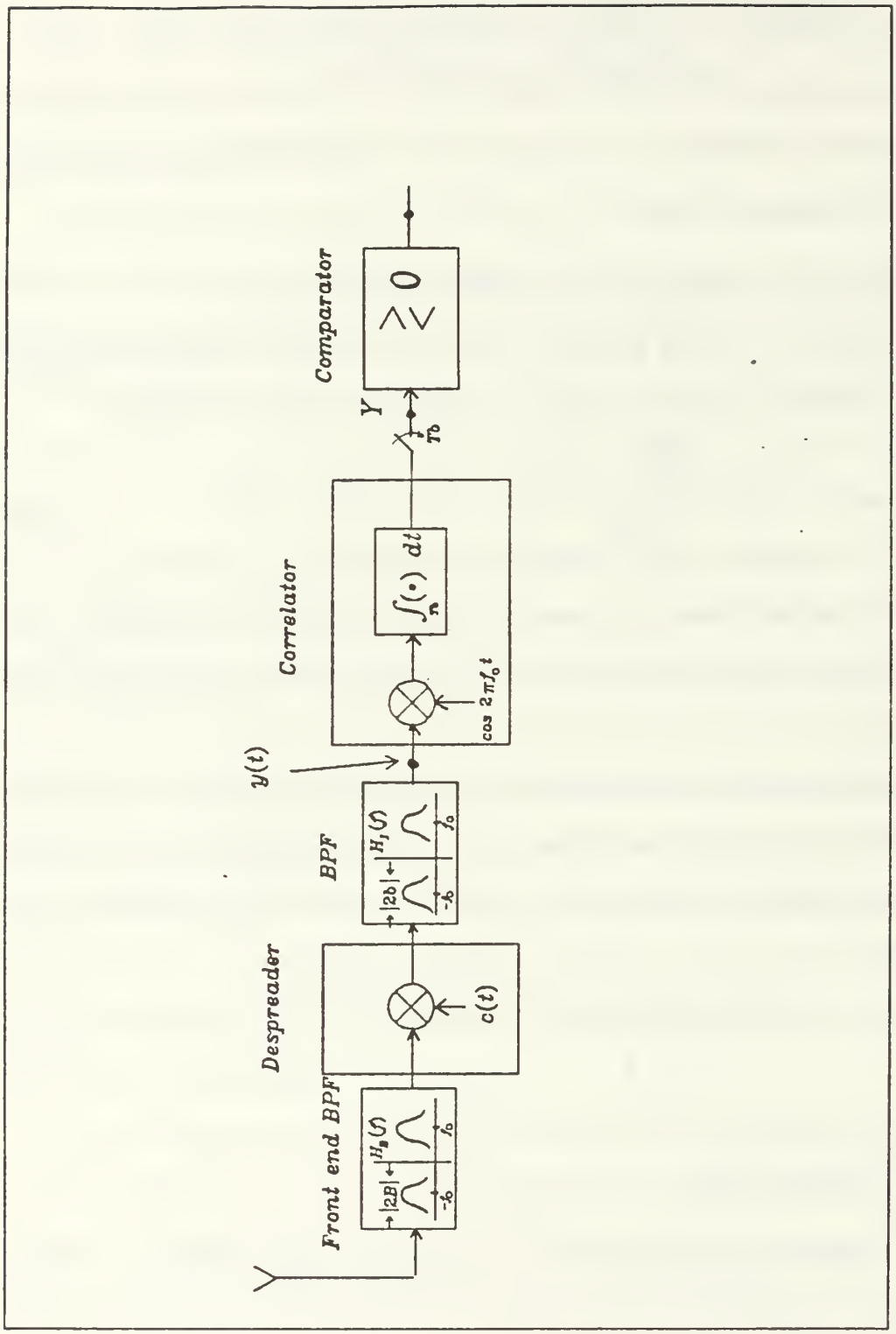

Figure 4.1 DS-BPSK Spread Spectrum Receiver

or simply,

$$Y = S_i + N_{th} + Y_J \tag{4.4}$$

where S_i, N_{th} and Y_J represents the three integrals in Equation 4.3 respectively. It is clear that Y is in fact a random variable whose statistics can be evaluated once certain properties of S_I, N_{th} and Y_J are established.

We first assume that the noise contribution at the front end of the receiver is zero mean, white Gaussian noise with $\frac{N_o}{2}$ as its two sided power spectral density level [Fig. 4.2]. The autocorrelation function for the noise, ednoted $R_N(t,\tau)$ is

$$R_N(t,\tau) = \frac{N_o}{2}\delta(t-\tau) \tag{4.5}$$

where $\delta(t)$ is the Dirac Delta function. Based on these assumptions it is shown in Appendix H that N_{th} is also a zero mean, Gaussian random variable with variance σ_{th}^2 specified in the sequel. Due to the fact that the receiver is linear, the noise contribution at the output retains its Gaussian statistics. The expression for σ_{th}^2 is from App. H given by (Eq. H.18).

$$\sigma_{th}^2 = \frac{N_o T_b k}{2\pi} \tag{4.6}$$

where

$$k = 0.903$$

and

$$G_c = \frac{R_c}{R_b} \triangleq \text{ processing gain.}$$

It is shown that S_1 and S_2 are given by [Ref. 2]

$$S_1 = \sqrt{\frac{E_b T_b}{2}} \quad \text{and} \quad S_2 = \sqrt{\frac{E_b T_b}{2}} \tag{4.7}$$

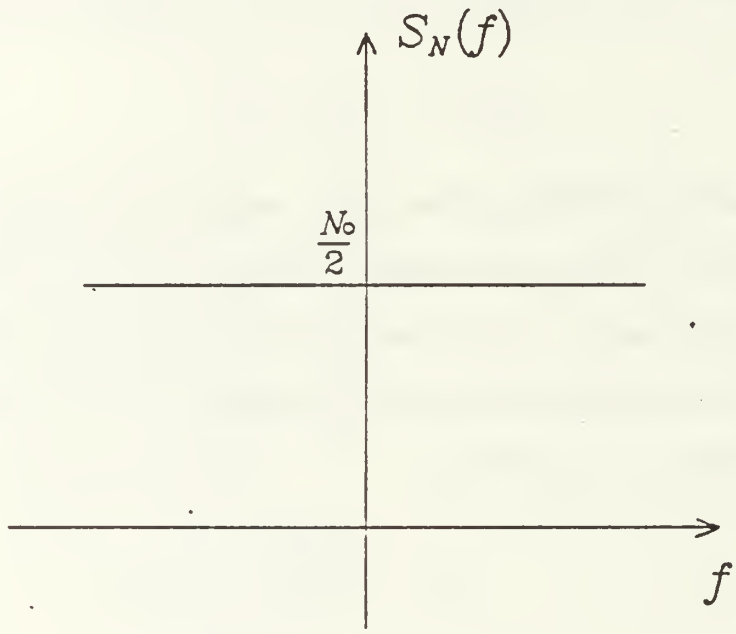

Figure 4.2 Power Spectral Density of the Thermal Noise

Furthermore, Y_J is the quantity related to the jammer and its variance σ_J^2 is given by (see Eq. H.4)

$$\sigma_J^2 = \frac{C_o T_b}{8} J(G_c)$$

where $J(G_c)$ is defined by Eq. 4.6. To further simplify the notation, let $X = N_{th} + Y_J$, so that

$$\sigma_X^2 = \sigma_{th}^2 + \sigma_J^2 \tag{4.7}$$

since the noise and jamming are zero mean uncorrelated processes, and

$$Y = S_i + X \tag{4.8}$$

then X is zero mean Gaussian random variable with pdf given by [Ref. 2]

$$f_x(X) = \frac{1}{\sqrt{2\pi\sigma_X^2}} e^{-\frac{x^2}{\sigma_X^2}} \tag{4.9}$$

For the BPSK modulation scheme that is being considered here, the decision regions of the signal space diagram can be illustrated as shown in Fig. 4.3 [Ref 4]: From equations 4.8 and 4.9, it can be seen that the probability of receiving the signal Y given that a signal S_i was actually transmitted is:

$$Pr\{r = Y/S_i(t) \text{ was transmitted}\} = f_{r/s_i}(Y/S_i) = f_x(Y - S_i) \tag{4.10}$$

The probability of bit error rate is then given by: [Ref. 2]

$$P_b = Q\left(\sqrt{\frac{E_b T_b}{2\sigma_X^2}}\right)$$

or

$$P_b = Q\left(\sqrt{\frac{E_b T_b}{2(\sigma_{th}^2 + \sigma_J^2)}}\right) \tag{4.11}$$

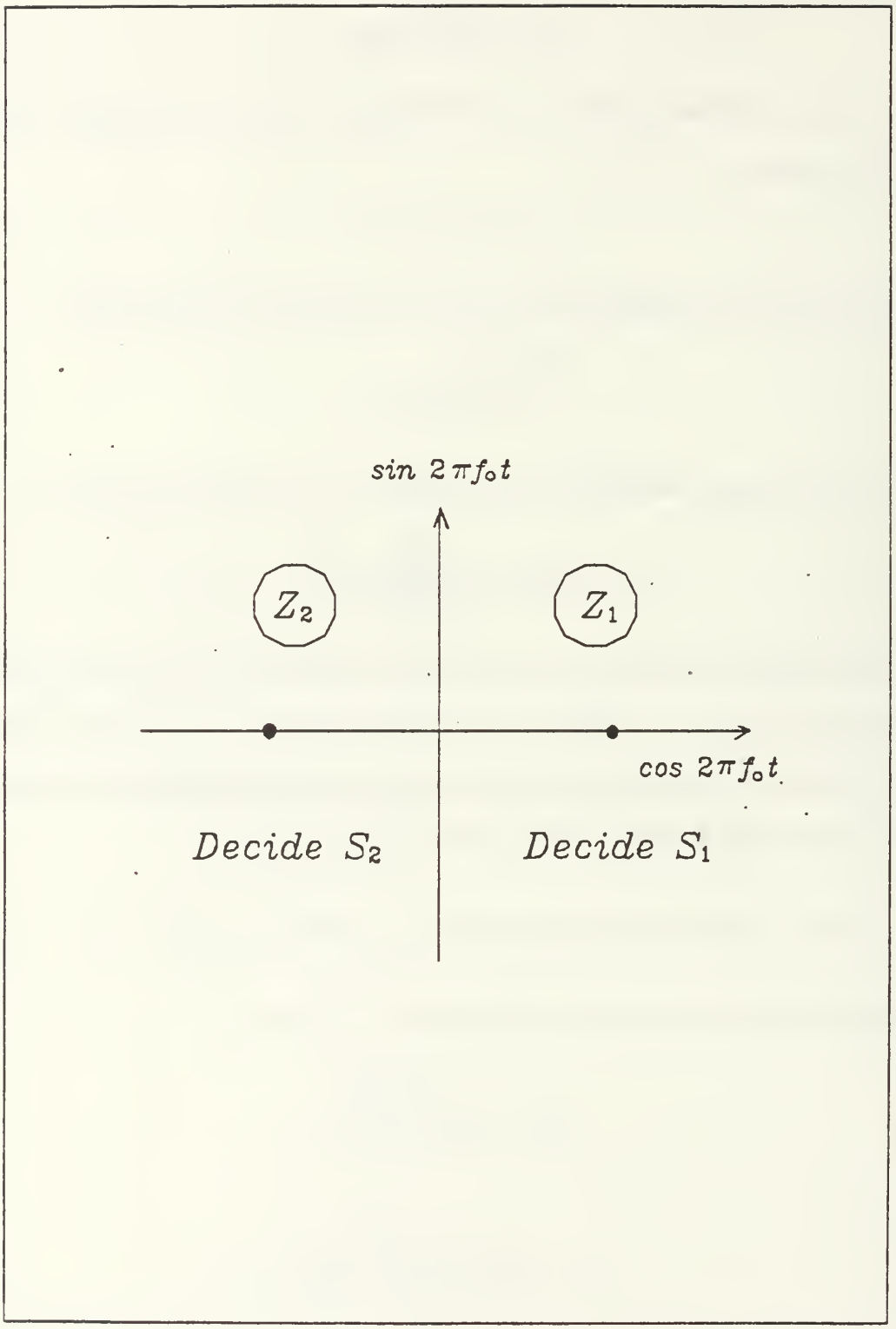

Figure 4.3 Signal Space Diagram for BKSP Modulation

where $Q(\cdot)$ is the complementary error function defined earlier in Chapter III. Substituting σ_{th}^2 and σ_J^2 from Equations H.4 and H.18 results in

$$P_b = Q\left(\sqrt{\frac{E_b T_b}{\frac{N_o T_b k}{\pi} + \frac{C_o T_b}{4} J(G_c)}}\right)$$

or

$$P_b = Q\left(\sqrt{\frac{E_b}{\frac{N_o k}{\pi} + \frac{C_o J(G_c)}{4}}}\right) \tag{4.12}$$

C. ANALYSIS OF ERROR PERFORMANCE

As derived in the previous section, Eq. 4.16 yields the probability of bit error P_b for a DS-BPSK spread spectrum receiver under AWGN noise interference and narrowband bi-level fast pulsed noise jamming. Clearly P_b is a function of the power spectral density level N_o of the AWGN, the average power of the jammer given by BC_o and also, the processing gain G_c. It is clear from Eq. 4.11 that the receiver bit error probability will increase if the noise and/or jammer power increases as the $Q(\cdot)$ function is monotonically decreasing.

In order to analyze the quantity P_b in more detail, we define the signal to noise ratio (SNR) to be the ratio of E_b to N_o and the jammer power to signal power ratio (JSR) to be the ratio of average jammer power P_J to the average signal power P [Ref. 4]. Hence,

$$SNR \triangleq \frac{E_b}{N_o} \quad , JSR \triangleq \frac{P_J}{P} \tag{4.17}$$

where

$$P_J = BC_o = 2\pi R_c C_o \tag{4.18}$$

$$P = E_b R_b \tag{4.19}$$

so that Eq. 4.16 can be reexpressed as

$$P_b = Q\left(\sqrt{\frac{SNR}{\frac{0.903}{\pi} + \frac{(JSR)(SNR)}{8\pi G_c}}}\right) \tag{4.20}$$

Based on Eq. 4.20, families of curves of P_b versus SNR for fixed JSR values can be plotted and analyzed. However, first plots of P_b versus JSR for different values of G_c under various SNR conditions are shown. Logarithm scales are used for P_b due to the large variation in this parameter. From Figure 4.4a to d, one can observe that in general, under intense jamming (i.e., JSR large), the receiver probability of error is also large, thus implying that a significant number of delivered data bits are in error. Under a fixed JSR and fixed G_c values, it can be seen that if the SNR is large, P_b can be made significantly small. For example in Fig. 4.4b, it is shown that when JSR = 15dB and G_c =100;

$$P_b(\text{at } SNR = 4) \approx 10^{-2.7}$$

and

$$P_b(\text{at } SNR = 20) \approx 10^{-20}$$

However, when the jamming is very strong (for JSR > 30 dB) P_b tends to a limit of approximately 10^{-1} regardless of the value of all other factors. It can be observed from Eq. 4.16 that if JSR increases indefinitely, the limit of P_b equal to 0.5 is reached.

From Fig. 4.4a to d, we can also conclude that for any fixed values of JSR and SNR, an increasing processing gain G_c implies a decreasing value of P_b. The phenomenon is more prominent in a high SNR environment than in a low SNR environment. There is no significant improvement in P_b for SNR in the range from 0 dB to 8 dB however a large improvement in P_b is obtained when SNR exceeds

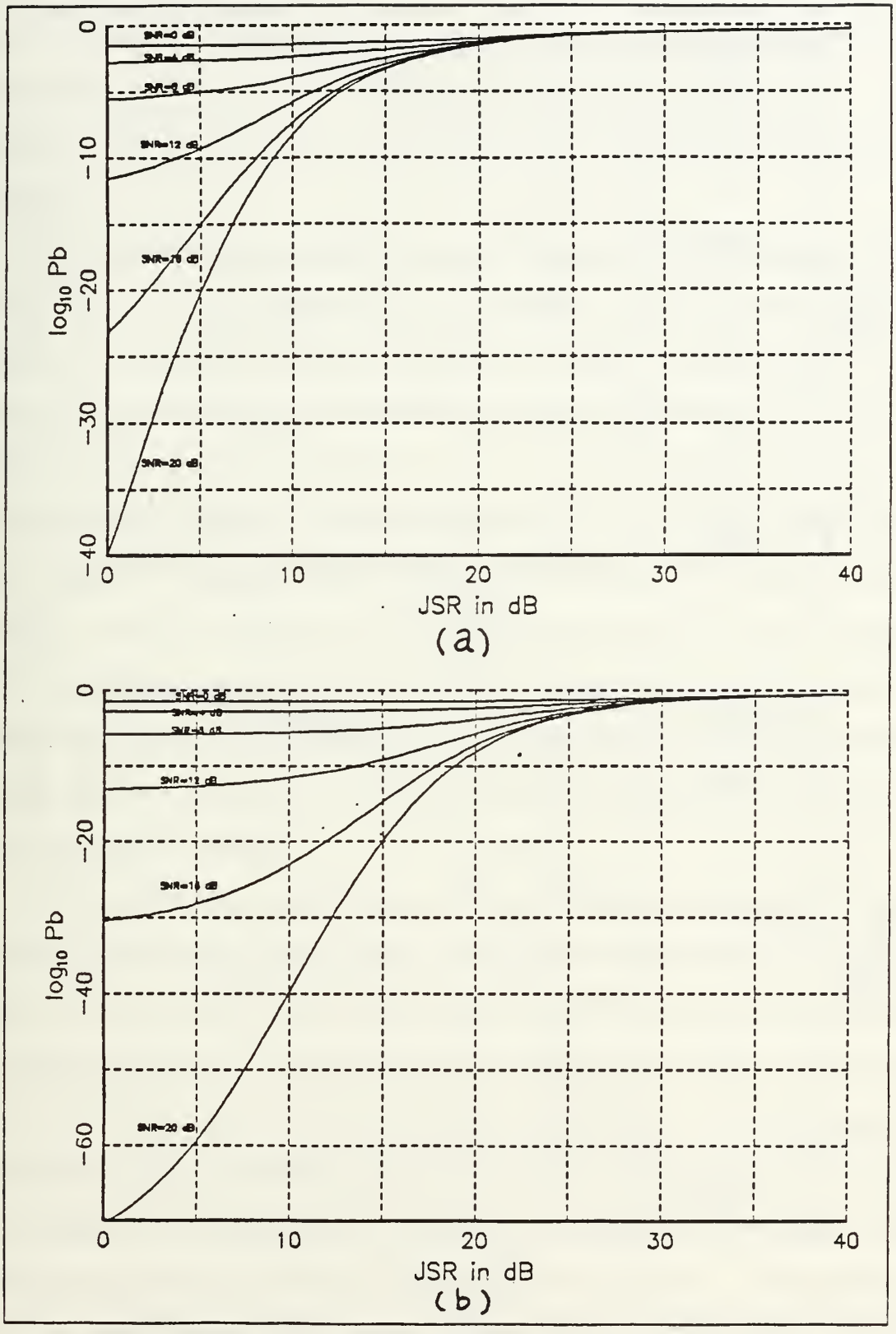

Figure 4.4 Pb versus JSR for (a) Gc=10
(b) Gc=100

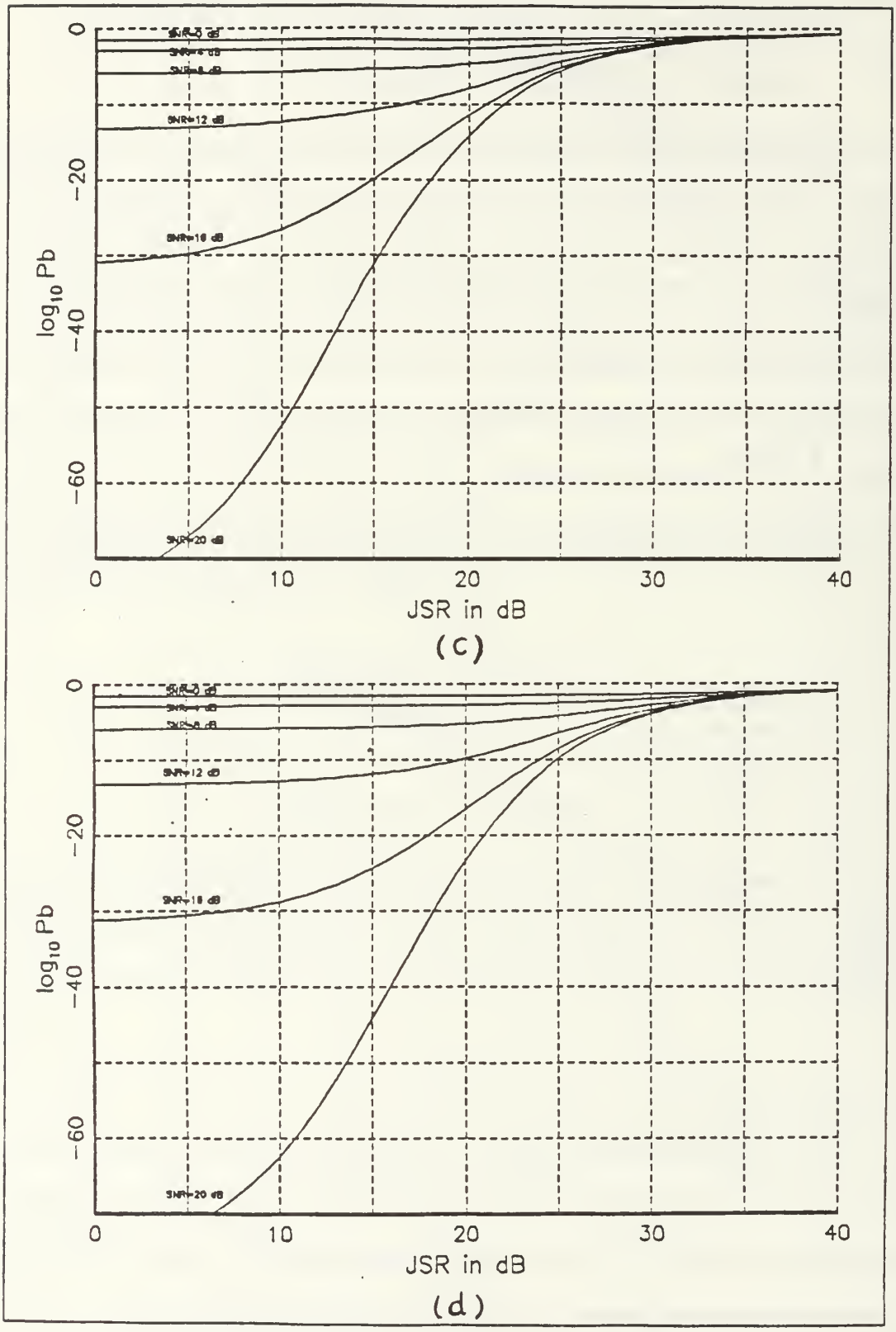

Figure 4.4 Pb versus JSR for (c) Gc=200
(d) Gc=400

12 dB. The immediate conclusion that we can draw from this is that by increasing the chip rate (R_c) of the spreading code, resulting in a higher processing gain, the perfromance of the receiver can be improved under the jamming environment analyzed, however this counter measure loses effectiveness when powerful jamming is present.

To better illustrate the effect of G_c on P_b, another family of curves is plotted. In Fig. 4.5a to d the variation of P_b as a function of JSR is shown for different values of G_c and SNR. It is clearly shown that all the curves converge toward P_b equal to 0.5 as JSR increases. From Fig. 4.5a we can see that P_b (at JSR = 20 dB) reduces from approximately $10^{-0.7}$ to $10^{-1.5}$ when G_c increases from 2 to 400 under weak signal (SNR = 4 dB) conditions, while P_b reduces from approximately $10^{-0.7}$ to 10^{-23} under the same conditions when SNR = 20 dB (see Fig. 4.5d). At JSR > 35 dB, no significant gain can be obtained regardless of signal strength. As a result of this, we can conclude that by increasing the chip rate to counter the narrowband bi-level fast pulsed noise jammer is not effective under strong jamming conditions, however, a high chip rate can reduce the probability of bit error of the jamming is not too severe.

It is also possible to represent the error performance curves by plotting $\log_{10} P_b$ versus SJR, the signal power to jammer power ratio under various SNR conditions. Fig. 4.6 a to d show how P_b varies with SJR. The curves can be interpreted in essentially the same way as the previously mentioned graphs. By comparing Fig. 4.6 a to d with the results obtained in Reference 2, we observe that the performance of the DS-BPSK spreak spectrum reciever degrades under a jamming environment in a manner similar to the case of barrage noise jamming or partial band noise jamming environment presented in the reference. Furthermore, the receiver performance is well below the boundary of the performance for the

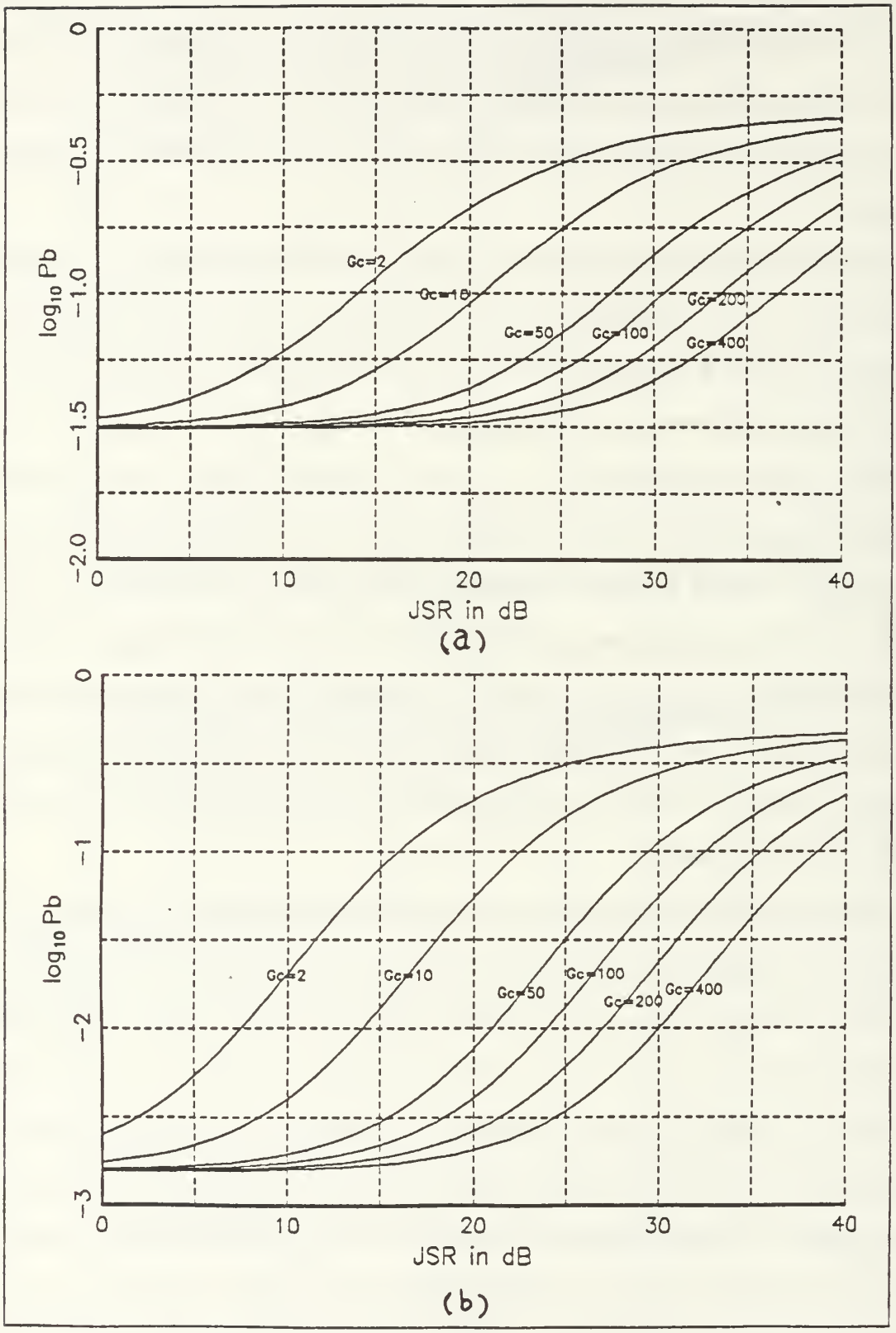

Figure 4.5 Pb versus JSR for (a) SNR=0 dB
(b) SNR=4 dB

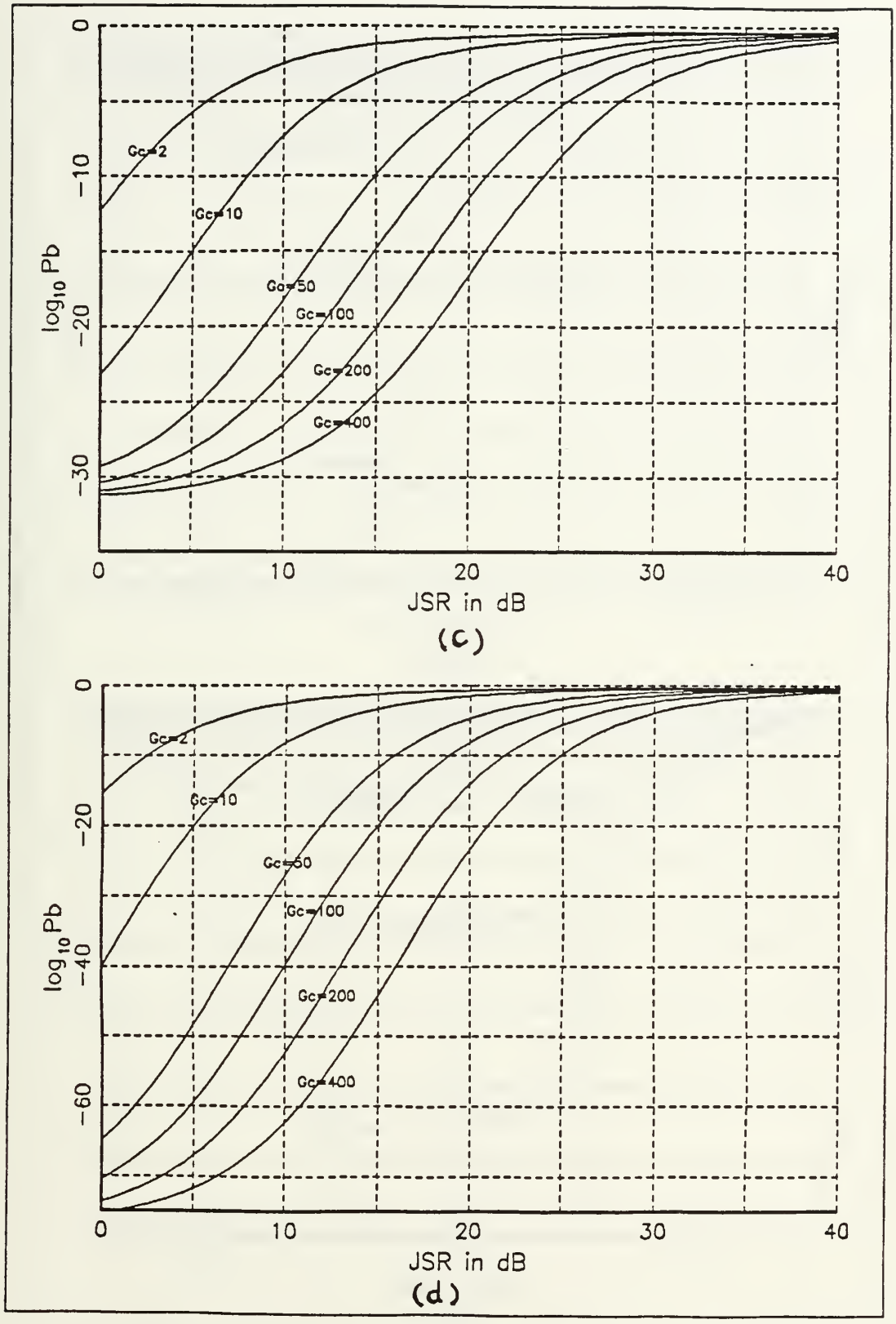

Figure 4.5 Pb versus JSR for (c) SNR=16 dB
(d) SNR=20 dB

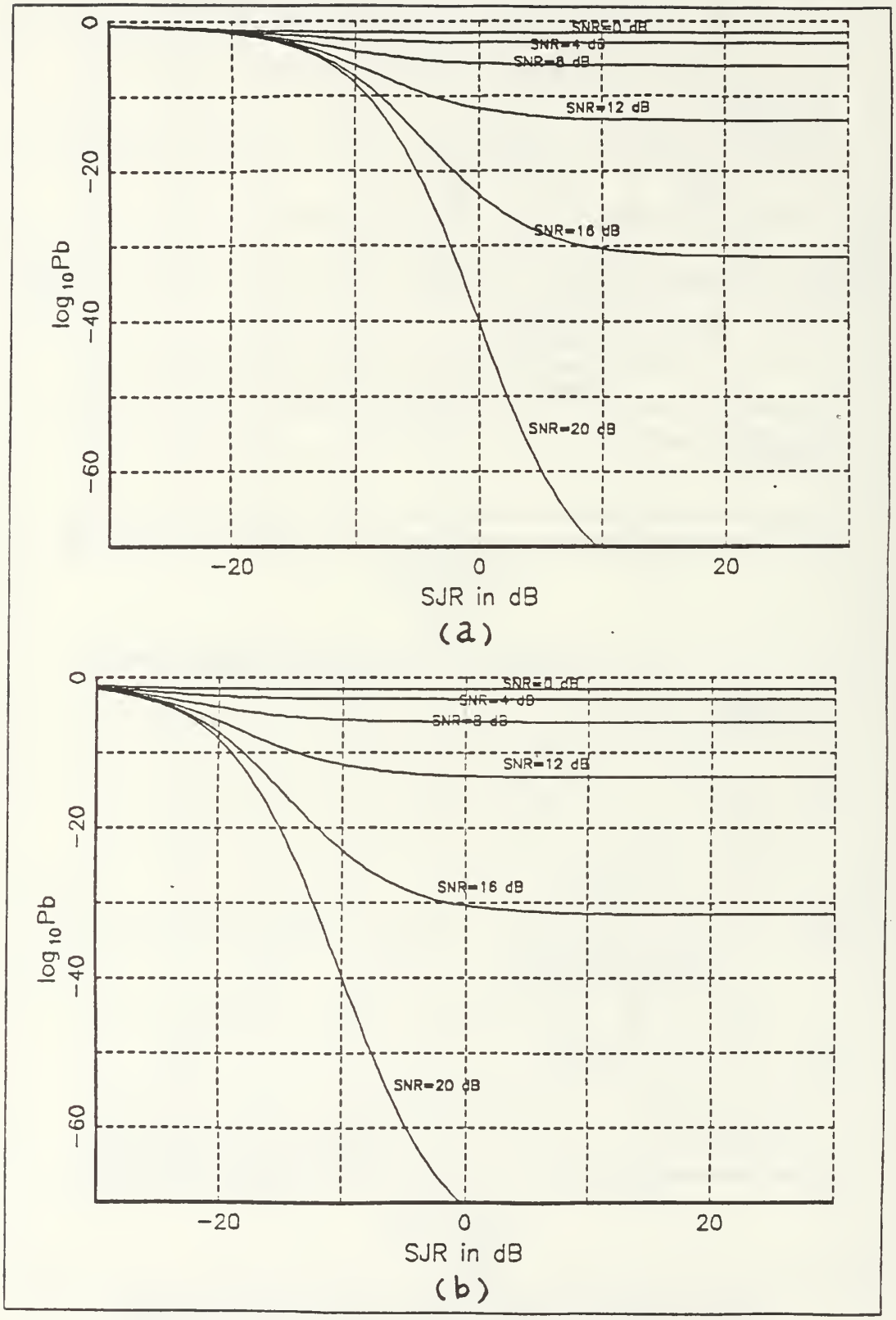

Figure 4.6 Pb versus SJR for (a) Gc=10
(b) Gc=100

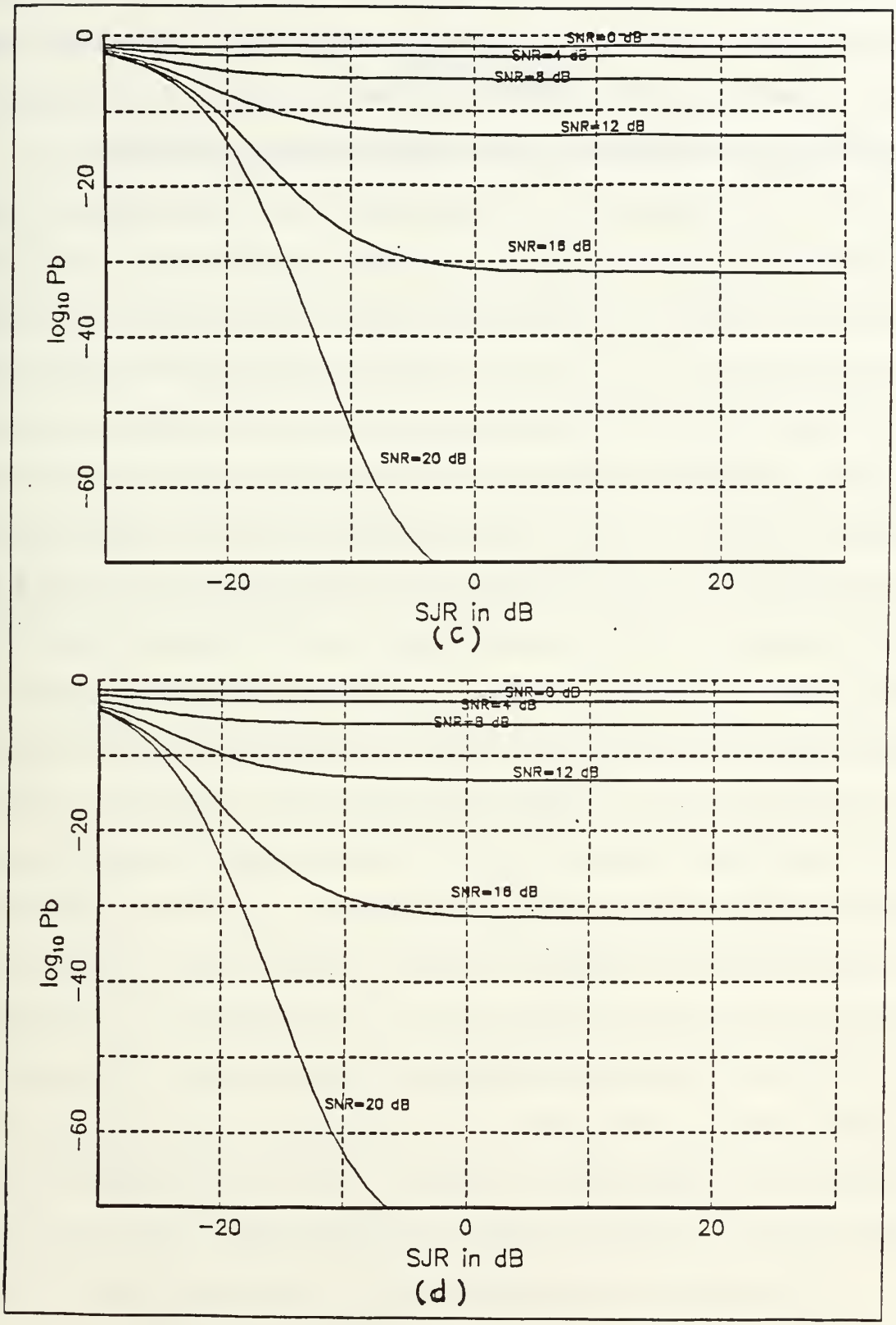

Figure 4.6 Pb versus SJR for (c) Gc=200
(d) Gc=400

worst case pulsed noise jamming derived in Reference 2 based on a quasi-stationary analysis method. Except for the weak signal condition case, the receiver performance approaches the above mentioned boundary. In general, by increasing the processing gain, the performance of the receiver improves significantly.

V. CONCLUSIONS

In this thesis it has been demonstrated that any nonstationary random process that is bandpass filtered can be represented in a mathematical form analogous to that used to represent narrowband wide sense stationary random processes. The quadrature components of the narrowband nonstationary process are themselves nonstationary low pass random processes. In general, the autocorrelation function of the two quadrature components are not identical and the cross-correlation function of the quadrature components is not necessarily an odd function. However, when the input nonstationary random process is real, the correlation functions of the quadrature components of the narrowband output process have properties similar to those associated with narrowband wide sense stationary random processes

The general representation of the nonstationary narrowband random process has been applied as a model for a specific class of electronic counter measure signals. Specifically a bi-level pulsed noise jammer, in which the power of the jammer periodically pulses between two levels is modeled using the previously mentioned nonstationary narrowband random process representation and its effect on a DS-BPSK receiver analyzed. This type of jammer was analyzed because it is quite effective in the sense that it produces significant performance degradations on the receiver. In practical cases, the jammer pulses between two levels at a rate faster than that of the data bit rate. The quasi-stationary analysis method for receiver performance is not valid. Therefore, a methodology has been developed that allows rather precise evaluation of receiver performance in terms of signal, noise, and jamming powers as well as spread spectrum processing gain.

The effect of the pulsed noise jammer on the spread spectrum binary phase shift keyed receiver was examined in detail and it is shown that a strong transmitted signal is more effective at mitigating the effect of the jammer than increasing the chip rate of the spreading code. The pulsed noise jamming can be shown to be quite effective under various signal power and processing gain values, as rather large bit error rates result when powerful jamming is present.

The thesis develops a methodology that can be used to evaluate the effect of a nonstationary narrowband random process interference on communication channels. There are two benefits from this study. First, in terms of ECM performance it makes it possible to evaluate the effectiveness of such jammers, and second, in terms of electronic counter counter measures (ECCM), the performance of jam resistant receivers can be evaluated more accurately. Although the example chosen in the study involves BPSK modulation spread by direct sequence methods, results for other forms of nonstationary jammings on different types of spread spectrum receivers can also be obtained from the above results with appropriate modification.

APPENDIX A

REPRESENTATION OF NARROWBAND FILTERS

Let

$$h_L(t) \overset{F}{\longleftrightarrow} H_L(f) = A(f)e^{j\theta(f)} \tag{A.1}$$

be the specification of a low-pass filter (LPF), and let

$$h_B(t) \overset{F}{\longleftrightarrow} H_B(f) = H_L(f - f_o) + H_L(-(f + f_o)) \tag{A.2}$$

where f_o is assumed to be much higher than the cutoff frequency of the LPF. Thus, $H_B(f)$ is the transfer function of a narrowband filter centered at $f = \pm f_o$. By inverse Fourier Transformation, we have:

$$\begin{aligned} h_B(t) &= \int_{-\infty}^{\infty} H_B(f)e^{j2\pi ft}df \\ &= \int_{-\infty}^{\infty} H_L(f - f_o)e^{j2\pi ft}df + \int_{-\infty}^{\infty} H_L(-f - f_0)e^{j2\pi ft}df \\ &= h_L(t)e^{j2\pi f_o t} + h_L(-t)e^{-j2\pi f_0 t} \end{aligned} \tag{A.3}$$

If we express

$$h_L(t) = h_{Lr}(t) + jh_{Li}(t)$$

since $h_L(t)$ may be complex, then

$$h_B(t) = [h_{Lr}(t) + h_{Lr}(-t)]\cos 2\pi f_o t + [h_{Li}(-t) - h_{Li}(t)]\sin 2\pi f_o t +$$

$$j\{[h_{Li}(t) + h_{Li}(-t)]\cos 2\pi f_o t + [h_{Lr}(-t) - H_{Lr}(-t)]\sin 2\pi f_o t\} \tag{A.4}$$

Since $h_B(t)$ will be assumed to be real, the imaginary part in Eq. A.4 must vanish, so that

$$h_{Li}(t) = -h_{Li}(-t) \quad \Longrightarrow \quad h_{Li} \text{ is an odd function.} \tag{A.5}$$

and

$$h_{Lr}(t) = h_{Lr}(-t) \quad \Longrightarrow \quad h_{Lr} \text{ is an even function.} \tag{A.6}$$

Observe also that

$$h_L(-t) = h_{Lr}(-t) + jh_{Li}(-t) = h_{Lr}(t) - jh_{Li}(t) = h_L^*(t) \tag{A.7}$$

Therefore

$$\begin{aligned} h_B(t) &= 2h_{Lr}(t)\cos 2\pi f_o t - 2h_{Li}(t)\sin 2\pi f_o t \\ &= h_L(t)e^{j2\pi f_o t} + [h_L(t)e^{j2\pi f_o t}]^* \end{aligned} \tag{A.8}$$

and finally

$$h_B(t) = 2\mathrm{Re}\left\{h_L(t)e^{j2\pi f_o t}\right\} \tag{A.9}$$

APPENDIX B

OUTPUT OF A NARROWBAND FILTER

The output $y(t)$ of a narrowband filter due to an input $x(t)$ is

$$\begin{aligned} y(t) &= \int_{-\infty}^{\infty} h_B(t-\alpha)x(\alpha)d\alpha \\ &= \int_{-\infty}^{\infty} \left[2h_{Lr}(t-\alpha)\cos 2\pi f_o(t-\alpha) - 2h_{Li}(t-\alpha)\sin 2\pi f_o(t-\alpha)\right] x(\alpha)d\alpha \end{aligned} \tag{B.1}$$

where the representation derived in App. A has been used to obtain Eq. B.1. By expanding $\cos 2\pi f_o(t-\alpha)$ and $\sin 2\pi f_o(t-\alpha)$ it is possible to obtain

$$y(t) = 2X_c(t)\cos 2\pi f_o t - 2X_s(t)\sin 2\pi f_o t \tag{B.2}$$

where

$$X_c(t) = \int_{-\infty}^{\infty} \left[h_{Lr}(t-\alpha)\cos 2\pi f_o\alpha + h_{Li}(t-\alpha)\sin 2\pi f_o\alpha\right] X(\alpha)d\alpha \tag{B.3}$$

and

$$X_s(t) = \int_{-\infty}^{\infty} \left[h_{Li}(t-\alpha)\cos 2\pi f_o\alpha - h_{Lr}(t-\alpha)\sin 2\pi f_o\alpha\right] X(\alpha)d\alpha \tag{B.4}$$

so that a standard narrowband-type representation is possible for the output $y(t)$. If $X(t)$ is a random process that is not necessarily stationary, $X_c(t)$ and $X_s(t)$ are themselves random processes with autocorrelation functions

$$\begin{aligned} R_c(t_1,t_2) &\triangleq E\left\{X_c(t_1)X_c(t_2)\right\} \\ &= \int_{-\infty}^{\infty}\int_{-\infty}^{\infty} \frac{1}{2}\left[h_L(t_1-\alpha)e^{j2\pi f_o\alpha} + h_L^*(t_1-\alpha)e^{-j2\pi f_o\alpha}\right] \\ &\cdot \frac{1}{2}\left[h_L(t_2-\beta)e^{j2\pi f_o\beta} + h_L^*(t_2-\beta)e^{-j2\pi f_o\beta}\right] R_x(\alpha,\beta)d\alpha d\beta \\ &= \frac{1}{2}\int_{-\infty}^{\infty}\int_{-\infty}^{\infty} \mathrm{Re}\left\{h_L^*(t_1-\alpha)h_L(t_2-\beta)e^{j2\pi f_o(\alpha+\beta)}\right\} R_x(\alpha,\beta)d\alpha d\beta + \end{aligned}$$

$$\frac{1}{2}\int_{-\infty}^{\infty}\int_{-\infty}^{\infty}\mathrm{Re}\left\{h_L^*(t_1,\alpha)h_L(t_2-\beta)e^{j2\pi f_o(\beta-\alpha)}\right\}R_x(\alpha,\beta)d\alpha d\beta \quad (B.5)$$

and

$$\begin{aligned}R_s(t_1,t_2) &\triangleq E\{X_s(t_1)X_s(t_2)\}\\ &= -\frac{1}{2}\int_{-\infty}^{\infty}\int_{-\infty}^{\infty}\mathrm{Re}\left\{h_L(t_1-\alpha)h_L(t_2-\beta)e^{-j2\pi f_o(\alpha+\beta)}\right\}R_x(\alpha,\beta)d\alpha d\beta+\\ &\frac{1}{2}\int_{-\infty}^{\infty}\int_{-\infty}^{\infty}\mathrm{Re}\left\{h_L^*(t_1-\alpha)h_L(t_2-\beta)e^{j2\pi f_o(\alpha-\beta)}\right\}R_x(\alpha,\beta)d\alpha d\beta\end{aligned} \quad (B.6)$$

The cross correlation functions are given by

$$\begin{aligned}R_{cs} &\triangleq E\{X_c(t_1)X_s(t_2)\}\\ &= \frac{1}{2}\int_{-\infty}^{\infty}\int_{-\infty}^{\infty}Im\left\{h_L(t_1-\alpha)h_L(t_2-\beta)e^{j2\pi f_o(\alpha-\beta)}\right\}R_x(\alpha,\beta)d\alpha d\beta+\\ &\frac{1}{2}\int_{-\infty}^{\infty}\int_{-\infty}^{\infty}Im\left\{h_L^*(t_1-\alpha)h_L(t_2-\beta)e^{-j2\pi f_o(\alpha+\beta)}\right\}R_x(\alpha,\beta)d\alpha d\beta\end{aligned} \quad (B.7)$$

and

$$\begin{aligned}R_{sc}(t_1,t_2) &\triangleq E\{X_s(t_1)X_c(t_2)\}\\ &= \frac{1}{2}\int_{-\infty}^{\infty}\int_{-\infty}^{\infty}Im\left\{h_L^*(t_1-\alpha)h_L(t_2-\beta)e^{-j2\pi f_o(\alpha-\beta)}\right\}R_x(\alpha,\beta)d\alpha d\beta+\\ &-\frac{1}{2}\int_{-\infty}^{\infty}\int_{-\infty}^{\infty}Im\left\{h_L^*(t_1-\alpha)h_L(t_2-\beta)e^{j2\pi f_o(\alpha+\beta)}\right\}R_x(\alpha,\beta)d\alpha d\beta\end{aligned} \quad (B.8)$$

Observe that in general $X_c(t)$ and $X_s(t)$ normally labeled the quadrature components of the narrowband process $y(t)$ are not stationary in general. Nevertheless, the derived autocorrelations and cross correlations can be used to obtain the autocorrelation of the random process of $y(t)$, namely

$$
\begin{aligned}
R_y(t_1, t_2) &\triangleq E\{y(t_1)y(t_2)\} \\
&= E\Big\{2[X_c(t_1)\cos 2\pi f_o t_1 - X_s(t_1)\sin 2\pi f_o t_1] \\
&\cdot 2[X_c(t_2)\cos 2\pi f_o t_2 - X_s(t_2)\sin 2\pi f_o t_2]\Big\} \\
&= 4\Big[R_c(t_1, t_2)\cos 2\pi f_o t_1 \cos 2\pi f_o t_2 + R_s(t_1, t_2)\sin 2\pi f_o t_1 \sin 2\pi f_o t_2 + \\
&- R_{cs}(t_1, t_2)\cos 2\pi f_o t_1 \sin 2\pi f_o t_2 \\
&- R_{sc}(t_1, t_2)\sin 2\pi f_o t_1 \cos 2\pi f_o t_2\Big] \qquad (B.9)
\end{aligned}
$$

APPENDIX C

NARROWBAND PROCESS AUTOCORRELATION FUNCTION EXAMPLE

The autocorrelation functions determined in Appendix B are now used to treat a specific case, namely when the input process $X(t)$ to the narrowband filter is generated by the system of Fig. 2.3. The resulting output $y(t)$ is a narrowband process bearing quadrature components whose autocorrelation function is given by (see Eq. 2.17)

$$R_c(t_1,t_2) = \frac{1}{2}\int_{-\infty}^{\infty} \mathrm{Re}\left\{h_L(t_1-\alpha)h_L(t_2-\alpha)e^{+j2\pi\cdot 2f_o\alpha}\right\} q_s(\alpha)d\alpha + \frac{1}{2}\int_{-\infty}^{\infty} \mathrm{Re}\left\{h_L^*(t_1-\alpha)h_L(t_2-\alpha)\right\} q_s(\alpha)d\alpha \qquad (C.1)$$

Given that $h_L(\cdot)$ represents a low-pass system and $q_s(\alpha)$ would normally vary much more slowly than the frequency $2f_o$, it can be seen that integrals involving a $2f_o$ frequency are negligible resulting in further simplifications. Thus

$$R_c(t_1,t_2) = \frac{1}{2}\int_{-\infty}^{\infty} \mathrm{Re}\left\{h_L^*(t_1-\alpha)h_L(t_2-\alpha)\right\} q_s(\alpha)d\alpha \qquad (C.2)$$

and similarly

$$R_s(t_1,t_2) = \frac{1}{2}\int_{-\infty}^{\infty} \mathrm{Re}\left\{h_L^*(t_1-\alpha)h_L(t_2-\alpha)\right\} q_s(\alpha)d\alpha = R_c(t_1,t_2) \qquad (C.3)$$

The crosscorrelations are given by

$$R_{cs}(t_1,t_2) = \frac{1}{2}\int_{-\infty}^{\infty} Im\left\{h_L(t_1-\alpha)h_L(t_2-\alpha)\right\} q_s(\alpha)d\alpha = R_{sc}(t_1,t_2). \qquad (C.4)$$

For the special case where $h_L(t)$ is real, $R_{cs}(t_1, t_2)$ and $R_{sc}(t_1, t_2)$ are both equal to zero, so that from Eq. B.9 and Eqs. C.2 and C.3, $R_y(t_1, t_2)$ becomes

$$\begin{aligned} R_y(t_1, t_2) &= 4R_c(t_1, t_2)\left[\cos 2\pi f_o t_1 \cos 2\pi f_o t_2 + \sin 2\pi f_o t_1 \sin 2\pi f_o t_2\right] \\ &= 4R_c(t_1, t_2)\cos 2\pi f_o(t_2 - t_1) \end{aligned} \tag{C.5}$$

and finally

$$R_y(t_1, t_2) = 2\cos 2\pi f_o(t_2 - t_1)\int_{-\infty}^{\infty} h_L(t_1 - \alpha)h_L(t_2 - \alpha)q_s(\alpha)d\alpha \tag{C.6}$$

APPENDIX D

AUTOCORRELATION FUNCTION AND AVERAGE POWER AT THE OUTPUT OF A NARROWBAND FILTER DUE TO A BI-LEVEL PULSED JAMMER

When $q(t)$ is a bi-level signal as shown in Fig. 2.5, it is clear that

$$q_s(t) = A^2 - \left\{(A^2 - c^2) \sum_{k=-\infty}^{\infty} [U(t - kT_q - \rho T_q) - U(t - kT_q - T_q)]\right\} \qquad (D.1)$$

where $U(t)$ is the unit step function. Let

$$I(t) \triangleq \int_{-\infty}^{\infty} h_L(t_1 - \alpha) h_L(t_2 - \alpha) q_s(\alpha) d\alpha$$

This integral must be determined in order to evaluate $R_y(t_1, t_2)$ as given by Eq. C.6. Substituting $q_s(t)$ into $I(t)$ and utilizing the one pole filter specification for $h_L(t)$ having 3 dB cutoff B *rps*, we get

$$\begin{aligned} I(t) = \frac{A^2 B}{2} e^{-B(t_1+t_2)} e^{2B\,\mathrm{Min}(t_1,t_2)} - B^2(A^2 - C^2) e^{-B(t_1+t_2)} \\ \left[\int_{-\infty}^{\infty} e^{2B\alpha} U(t_1 - \alpha) U(t_2 - \alpha) \sum_{k=-\infty}^{\infty} U(\alpha - kT_q - \rho T_q) d\alpha \right. \\ \left. - \int_{-\infty}^{\infty} e^{2B\alpha} U(t_1 - \alpha) U(t_2 - \alpha) \sum_{k=-\infty}^{\infty} U(\alpha - kT_q - T_q) d\alpha\right] \end{aligned} \qquad (D.2)$$

The remaining integrals in Eq. D.2 are:

$$\begin{aligned} \sum_{k=-\infty}^{\infty} \int_{(k-\rho)T_q}^{\mathrm{Min}(t_1,t_2)} e^{2B\alpha} d\alpha &= \frac{1}{2B} \sum_{k=-\infty}^{[s]} \left[e^{2B\,\mathrm{Min}(t_1,t_2)} - e^{2B(k+1)T_q}\right] \\ &\quad \text{if } (k+1)T_q < \mathrm{Min}(t_1, t_2) \\ &= 0 \qquad \text{otherwise} \end{aligned} \qquad (D.3)$$

and

$$\sum_{k=-\infty}^{\infty} \int_{(k-1)T_q}^{\mathrm{Min}(t_1,t_2)} e^{2B\alpha}\, d\alpha = \frac{1}{2B} \sum_{k=-\infty}^{[s]} \left[e^{2B\,\mathrm{Min}(t_1,t_2)} - e^{2B(k+1)T_q} \right]$$
$$\text{if } (k+1)T_q < \mathrm{Min}(t_1,t_2) \qquad (D.4)$$
$$= 0 \qquad \text{otherwise}$$

where $[z]$ = largest integer less than or equal to z and

$$r = -e + \frac{1}{T_q}\mathrm{Min}(t_1,t_2) \quad ; \quad s = 1 + \frac{1}{T_q}\mathrm{Min}(t_1,t_2) \qquad (D.5)$$

The difference of the two integrals given by Eq. D.3 and D.4 produces

$$\frac{1}{2B}\left\{ \sum_{k=-\infty}^{[r]} \left[e^{2B\,\mathrm{Min}(t_1,t_2)} - e^{2B(k+\rho)T_q} \right] - \sum_{k=-\infty}^{[s]} \left[e^{2B\,\mathrm{Min}(t_1,t_2)} - e^{2B(k+1)T_q} \right] \right\} \qquad (D.6)$$

since $0 < \rho \leq 1$, we have $r \geq s$, so that

$$\sum_{k=-\infty}^{[r]} e^{2B\,\mathrm{Min}(t_1,t_2)} - \sum_{k=-\infty}^{[s]} e^{2B\,\mathrm{Min}(t_1,t_2)} = e^{2B\,\mathrm{Min}(t_1,t_2)}\,[[r]-[s]] \qquad (D.7)$$

Furthermore

$$\sum_{k=-\infty}^{[s]} e^{2B(k+1)T_q} - \sum_{k=-\infty}^{[r]} e^{2B(k+\rho)T_q} = \frac{e^{2BT_q} \cdot e^{2BT_q[s]} - e^{2B\rho T_q} \cdot e^{2BT_q[r]}}{1 - e^{-2BT_q}} \qquad (D.8)$$

Combining the above results yields (see Eq. C.6)

$$\begin{aligned} R_y(t_1,t_2) &= 2\cos 2\pi f_o t \cdot I(t) \\ &= 2\cos 2\pi f_o t \left\{ \frac{A^2 B}{2} e^{-B(t_1+t_2)} e^{2B\,\mathrm{Min}(t_1,t_2)} - \right. \\ &\frac{B(A^2-c^2)}{2} e^{-B(t_1+t_2)} \left[e^{2B\,\mathrm{Min}(t_1,t_2)} \Big([r]-[s] \Big) \right. \\ &\left. \left. + \frac{e^{2BT_q} e^{2BT_q[s]} - e^{2B\rho T_q} e^{2BT_q[r]}}{1 - e^{-2BT_q}} \right] \right\} \end{aligned} \qquad (D.9)$$

Since $X(t)$ represents a bi-level pulsed jammer, the power due to the jammer at the output of the narrowband filter denoted by P_J can be obtained by letting $t_1 = t_2 = t$ in the expression of $R_y(t_1, t_2)$ and time averaging the result. Thus

$$R_y(t,t) = A^2 B - B(A^2 - C^2)([r] - [s]) - \frac{B(A^2 - C^2)}{1 - e^{-2BT_q}} \Big[e^{2BT_q} e^{-2B(t - T_q[s])} - e^{2B\rho T_q} e^{-2B(t - T_q[r])} \Big] \tag{D.10}$$

which must now be time averaged in order to obtain P_J, the average jammer power. With the aid of Diagram D.1, D.2, and D.3 we note that all the three functions $\{[r] - [s]\}, \{t - T_q[s]\}$ and $\{t - T_q[r]\}$ are functions of t, and their time average values can be calculated as follows:

$$\begin{aligned} \overline{([r] - [S])} &= \lim_{n \to \infty} \left(\frac{1}{nT_q} [T_q + (n-1)(1-\rho)T_q] \right) \\ &= \lim_{n \to \infty} \frac{1}{n} [\rho + (1-\rho)n] = 1 - \rho \end{aligned} \tag{D.11}$$

$$\overline{e^{-2B(t - T_q[S])}} = \lim_{n \to \infty} \frac{1}{nT_q} \int_0^{T_q} n e^{-2B(t + t_q)} = \frac{e^{-2BT_q}}{2BT_q} (1 - e^{-2BT_q}) \tag{D.12}$$

$$\begin{aligned} \overline{e^{-2B(t - T_q[r])}} &= \lim_{n \to \infty} \frac{1}{(n+\rho)T_q} \left[\int_0^{\rho T_q} e^{-2Bt} dt + n \int_0^{T_q} e^{-2B(t + \rho T_q)} dt \right] \\ &= \frac{e^{-2B\rho T_q} (1 - e^{-2BT_q})}{2BT_q} \end{aligned} \tag{D.13}$$

Therefore, the final expression for P_J is

$$\begin{aligned} P_J &= A^2 B - B(A^2 - C^2)(1 - \rho) - \frac{B(A^2 - C^2)}{1 - e^{-2BT_q}} \left[\frac{1 - e^{-2BT_q}}{2BT_q} - \frac{1 - e^{-2BT_q}}{2BT_q} \right] \\ &= B[A^2 \rho + C^2 (1 - \rho)] \end{aligned} \tag{D.14}$$

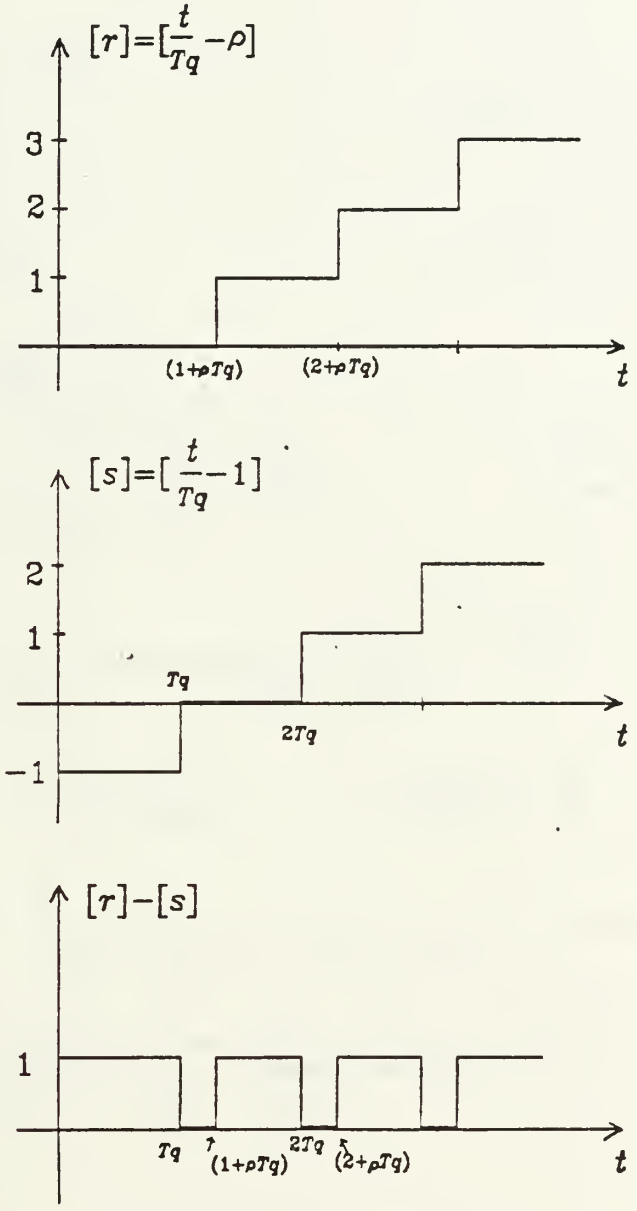

Figure D.1 Function [r]−[s]

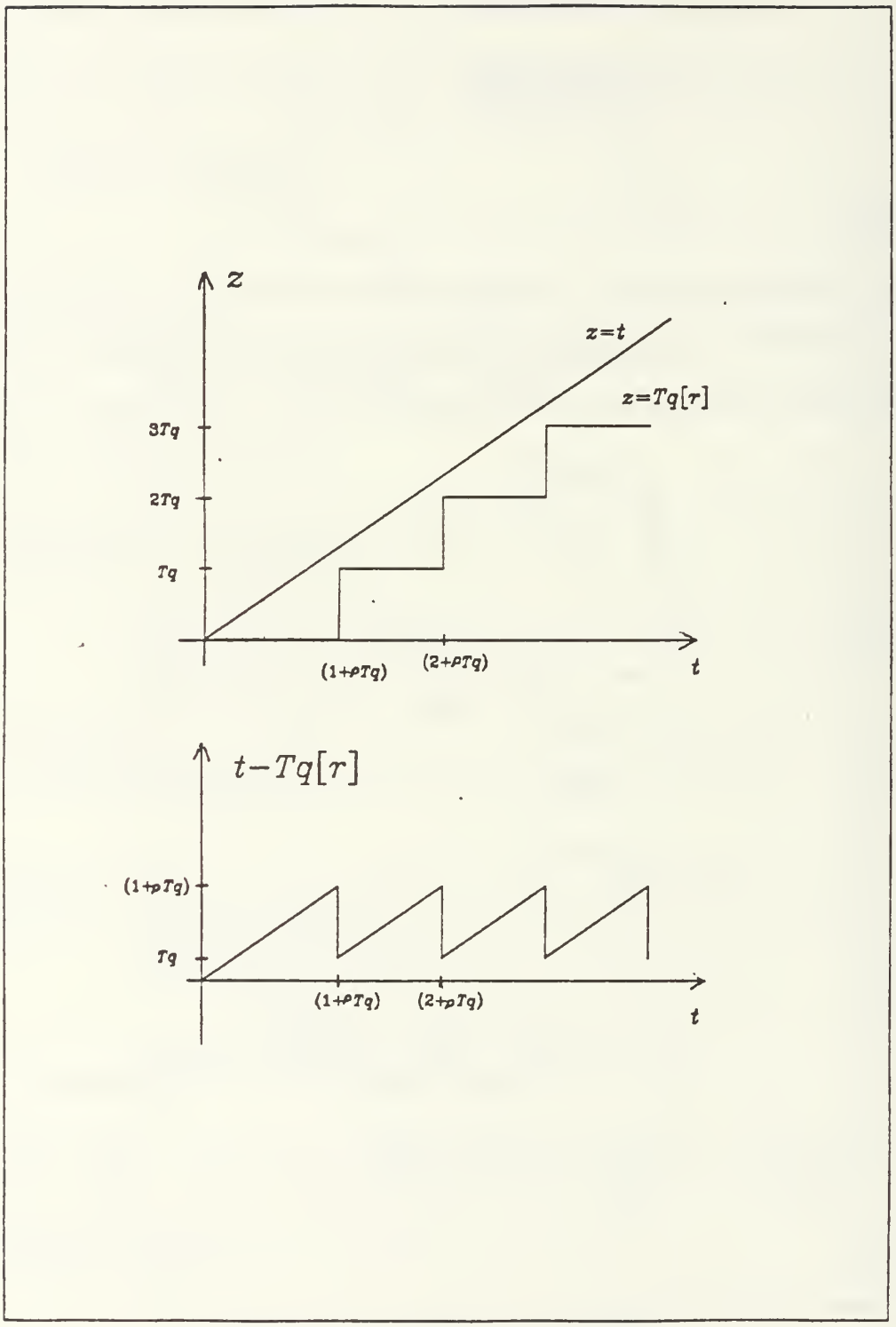

Figure D.2 Function (t−Tq[r])

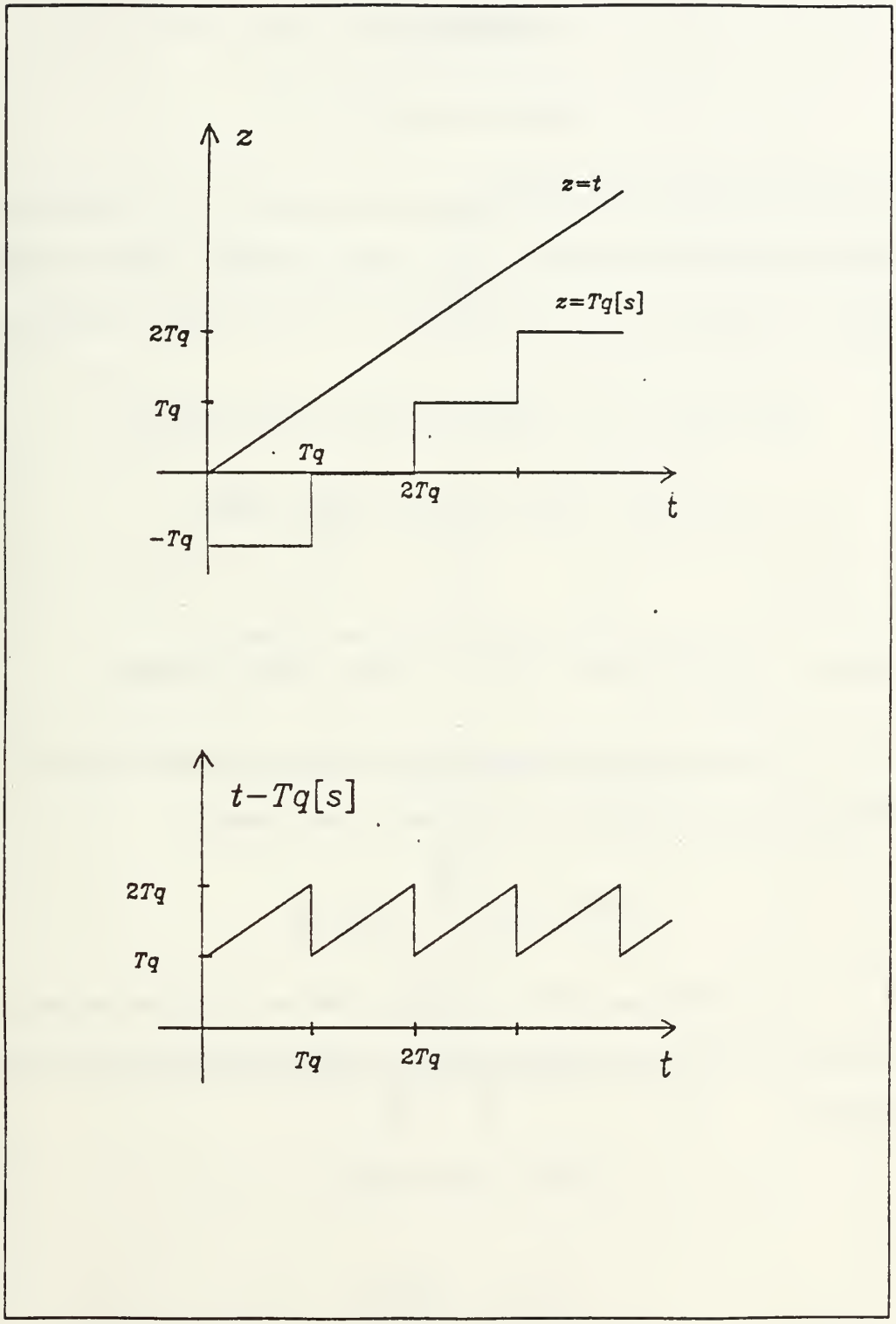

Figure D.3 Function (t−Tq[s])

APPENDIX E

VARIANCE OF Y_J

Since $y(t)$ is Gaussian and zero mean random process, Y_J is a Gaussian, zero mean random variable due to the fact that linear operations only are applied to $y(t)$. [Ref 2] The variance of Y_J, denoted by σ_J^2 can therefore be expressed as follows:

$$\begin{aligned}\sigma_J^2 &= E\left\{\int_0^{T_b}\int_0^{T_b} z(t)z(v)\cos 2\pi f_0 t \cos 2\pi f_0 v dt dv\right\} \\ &= \int_0^{T_b}\int_0^{T_b} R_z(t,v)\cos 2\pi f_0 t \cos 2\pi f_0 v dt dv\end{aligned} \tag{E.1}$$

where

$$R_z(t,v) = \int_{-\infty}^{\infty}\int_{-\infty}^{\infty} h_I(t-\tau)h_I(v-\gamma)R_y(\tau,\gamma)R_c(\tau-\gamma)d\tau d\gamma \tag{E.2}$$

and $R_c(\tau-\gamma)$ is defined as the autocorrelation function of the spreading code. For DS-BPSK spreading modulation, $R_c(\delta)$ is well known, namely

$$R_c(\delta) = \begin{cases} 1-\frac{|\delta|}{T_c} & ;\ |\delta| < T_c \\ 0 & ;\ |\delta| \geq T_c \end{cases}$$

where T_c^{-1} is the digital rate of the spreading code and is called the chip rate. The power spectrum of the spreading code $S_c(f)$ is the Fourier transform of $R_c(\delta)$, namely [Ref. 2].

$$S_c(f) = T_c \mathrm{sinc}^2(fT_c) \tag{E.3}$$

where

$$\mathrm{sinc}(x) = \frac{\sin \pi x}{\pi x}$$

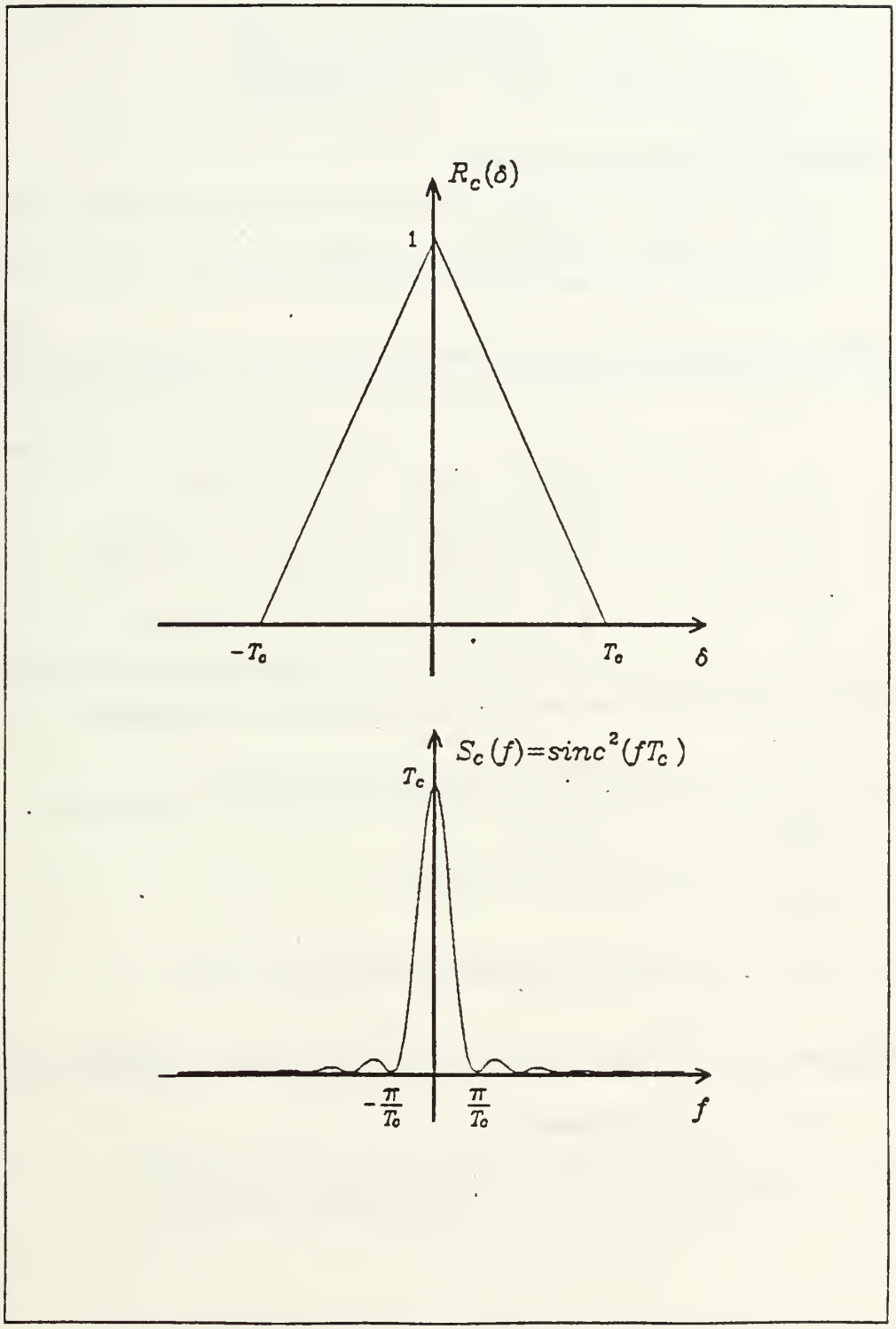

Figure E.1 Autocorrelation Function and Power Spectral Density of DS-BPSK Spreading Code

A diagram of $R_c(\delta)$ and $S_c(f)$ is shown in Fig. E.1.

A new signal $P_c(t)$ is defined as follows:

$$P_c(t) = \begin{cases} \cos 2\pi f_0 t & ; 0 \leq t \leq T_b \\ 0 & ; \text{otherwise} \end{cases}$$

So that equation E.1 can be rewritten as:

$$\sigma_J^2 = \int_{-\infty}^{\infty} \int_{-\infty}^{\infty} R_z(t,v) P_c(t) P_c(v) dt dv \qquad (E.4)$$

It is possible to express $R_z(t,v)$ as the double inverse Fourier transform of $S_Z(f,\nu)$, that is

$$R_z(t,v) = \int_{-\infty}^{\infty} \int_{-\infty}^{\infty} S_Z(f,\nu) e^{j2\pi(ft - v\nu)} df\, d\nu \qquad (E.5)$$

where

$$S_Z(f,\nu) = \int_{-\infty}^{\infty} \int_{-\infty}^{\infty} R_z(t,v) e^{-j2\pi(ft - v\nu)} dt dv \qquad (E.6)$$

Let $P_c(f)$ be the Fourier Transform of $P_c(t)$, so that Eq. E.2 becomes

$$\begin{aligned} \sigma_J^2 &= \int_{-\infty}^{\infty} \int_{-\infty}^{\infty} S_Z(f,\nu) \int_{-\infty}^{\infty} \int_{-\infty}^{\infty} P_c(t) e^{j2\pi f t} P_c(v) e^{-j2\pi\nu v} dt dv df d\nu \\ &= \int_{-\infty}^{\infty} \int_{-\infty}^{\infty} S_Z(f,\nu) P_c(-f) p_c(\nu) df d\nu \end{aligned} \qquad (E.7)$$

Using equation E.2 to evaluate equation E.6 results in

$$\begin{aligned} S_Z(f,\nu) = \int_{-\infty}^{\infty} \int_{-\infty}^{\infty} R_y(\tau,\gamma) R_c(\tau-\gamma) \int_{-\infty}^{\infty} \int_{-\infty}^{\infty} h_I(t-\tau) e^{-j2\pi f t} \cdot \\ h_I(v-\gamma) e^{j2\pi\nu v} dt dv d\tau d\gamma \cdot \\ = H_I(f) H_I(-\nu) \int_{-\infty}^{\infty} \int_{-\infty}^{\infty} R_y(\tau,\gamma) R_c(\tau-\gamma) d\tau d\gamma \end{aligned} \qquad (E.8)$$

since

$$\int_{-\infty}^{\infty} h_I(t-\tau) e^{-j2\pi f t} dt = H_I(f) e^{-j2\pi f \tau} \qquad (E.9)$$

and $H_I(f_0)$ is the Fourier Transform of $h_I(t)$. Therefore

$$\sigma_J^2 = \int_{-\infty}^{\infty}\int_{-\infty}^{\infty} H_I(f)H_I(-\nu)P_c(-f)P_c(\nu)\cdot \int_{-\infty}^{\infty}\int_{-\infty}^{\infty} R_y(\tau,\gamma)R_c(\tau-\gamma)e^{-j2\pi f\tau}e^{j2\pi\nu\gamma}\,d\tau\,d\gamma\,df\,d\nu \tag{E.10}$$

The double integration involving the variables τ and γ in equation E.10 can be evaluated for the special case where $y(t)$ is the nonstationary random process described previously.

In order to evaluate σ_J^2, the double integral $D(\tau,\gamma)$ defined as must first be evaluated, where

$$D(\tau,\gamma) = \int_{-\infty}^{\infty}\int_{-\infty}^{\infty} R_y(\tau,\gamma)R_c(\tau,\gamma)e^{-j2\pi f\tau}e^{j2\pi\nu\gamma}\,d\tau\,d\gamma \tag{E.11}$$

Recall from equation 2.20 that

$$R_y(\tau,\gamma) = 2\cos 2\pi f_0(\tau-\gamma)\eta(\tau,\gamma) \tag{E.12}$$

where

$$\eta(\tau,\gamma) = \int_{-\infty}^{\infty} h_L(\tau-\alpha)h_L(\gamma-\alpha)q_s(\alpha)\,d\alpha \tag{E.13}$$

The double Fourier transform pair $\eta(\tau,\gamma)$ and $H(u,w)$ can hence be expressed as:

$$H(u,w) = \int_{-\infty}^{\infty}\int_{-\infty}^{\infty} \eta(\tau,\gamma)e^{-j2\pi\tau u}e^{j2\pi\gamma w}\,d\tau\,d\gamma \tag{E.14}$$

so that

$$\eta(\tau,\gamma) = \int_{-\infty}^{\infty}\int_{-\infty}^{\infty} H(u,w)e^{-j2\pi\tau u}e^{j2\pi\gamma w}\,du\,dw \tag{E.15}$$

Therefore,

$$D(\tau,\gamma) = \int_{-\infty}^{\infty}\int_{-\infty}^{\infty} 2\left[\int_{-\infty}^{\infty}\int_{-\infty}^{\infty} H(u,w)e^{j2\pi\tau u}e^{-j2\pi\gamma w}\,du dw\right]\cdot$$
$$R_c(\tau-\gamma)\cos 2\pi f_0(\tau-\gamma)e^{-j2\pi f\tau}e^{j2\pi\nu\gamma}\,d\tau d\gamma$$
$$= \int_{-\infty}^{\infty}\int_{-\infty}^{\infty} H(u,w)\int_{-\infty}^{\infty}\int_{-\infty}^{\infty} 2R_c(\tau-\gamma)\cos 2\pi f_0(\tau-\gamma)\cdot$$
$$e^{-j2\pi(f-u)\tau}e^{-j2\pi(w-\nu)\gamma}\,d\tau d\gamma du dw$$
$$= \int_{-\infty}^{\infty}\int_{-\infty}^{\infty} H(u,w)\int_{-\infty}^{\infty}\left[S_c(f-u+f_0)+S_c(f-u-f_0)\right]$$
$$e^{-j2\pi(f-u)\gamma}e^{-j2\pi(w-\nu)\gamma}\,d\gamma du dw$$
$$= \int_{-\infty}^{\infty}\int_{-\infty}^{\infty} H(u,w)\left[S_c(f-u+f_0)+S_c(f-u-f_0)\right]\delta(f-u+w-\nu)\,du dw \qquad (E.16)$$

Carrying out the last integration with respect to w, results in

$$D(\tau,\gamma) = \int_{-\infty}^{\infty} H(u,u+\nu-f)\left[S_c(f-u+f_0)+S_c(f-u-f_0)\right]du \qquad (E.17)$$

Evaluation of $H(u,w)$ which is defined in Equation E.14, can be accomplished by performing a double Fourier transformation on $\eta(\tau,\gamma)$. The single Fourier transform of $\eta(\tau,\gamma)$ is

$$\int_{-\infty}^{\infty}\eta(\tau,\gamma)e^{-j2\pi u\tau}d\tau = \int_{-\infty}^{\infty} h_L(\gamma-\alpha)\int_{-\infty}^{\infty} h_L(\tau-\alpha)e^{-j2\pi u\tau}d\tau q_s(\alpha)d\alpha \qquad (E.18)$$

Since

$$\int_{-\infty}^{\infty} h_L(\tau-\alpha)e^{-j2\pi u\tau}d\tau = H_L(u)e^{-j2\pi u\alpha}$$

transforming again the left hand side of equation E.18, results in

$$\int_{-\infty}^{\infty}\int_{-\infty}^{\infty}\eta(\tau,\gamma)e^{-j2\pi u\tau}e^{j2\pi w\gamma}\,d\tau d\gamma = \int_{-\infty}^{\infty} H_L(u)q_s(\alpha)e^{-j2\pi u\alpha}\cdot$$
$$\int_{-\infty}^{\infty} h_L(\gamma-\alpha)e^{j2\pi w\gamma}\,d\gamma d\alpha$$

or

$$H(u,w) = H_L(u)H_L(-w)\int_{-\infty}^{\infty} q_s(\alpha)e^{-j2\pi(u-w)\alpha}\,d\alpha \qquad (E.19)$$

However, being a periodic deterministic signal, $q_s(\alpha)$ can be expressed in terms of its exponential Fourier series expasion as follows

$$q_s(\alpha) = \sum_{n=-\infty}^{\infty} C_n e^{j2\pi n \alpha R_q}$$

so that

$$\int_{-\infty}^{\infty} q_s(\alpha) e^{-j2\pi(u-w)\alpha} d\alpha = \sum_{n=-\infty}^{\infty} C_n \int_{-\infty}^{\infty} e^{j2\pi(nR_q - u + w)\alpha} d\alpha \qquad (E.20)$$

Evaluation of the C_n coefficients for a particular case of interest is worked out in Appendix F. Combining Equations E.19 and E.20 yields

$$H(u,w) = \sum_{n=-\infty}^{\infty} C_n H_L(u) H_L(-w) \delta(nR_q - u + w) \qquad (E.21)$$

From equation E-21, it is clear that

$$H(u, u+\nu-f) = H_L(u) H_L(f-\nu-u) \sum_{n=-\infty}^{\infty} C_n \delta(nR_q + \nu - f) \qquad (E.22)$$

Equation E.17 can hence be further simplified to yield:

$$\begin{aligned} D(\tau,\gamma) &= \int_{-\infty}^{\infty} \sum_{n=-\infty}^{\infty} C_n H_L(u) H_L(f-\nu-u) \delta(nR_q + \nu - f) \cdot \\ &\quad [S_c(f+f_0-u) + S_c(f-f_0-u)] du \\ &= \sum_{n=-\infty}^{\infty} C_n \delta(nR_q + \nu - f) \int_{-\infty}^{\infty} H_L(u) H_L(f-\nu-u) \cdot \\ &\quad [S_c(f+f_0-u) + S_c(f-f_0-u)] du \end{aligned} \qquad (E.23)$$

Observing that in the integrand of equation E.23, u is the variable of integration, we can define

$$H_L^I(f,\nu) \triangleq \int_{-\infty}^{\infty} H_L(u) H_L(f-\nu-u) [S_c(f+f_0-u) + S_c(f-f_0-u)] du \qquad (E.24)$$

Substituting now $D(\tau,\gamma)$ in equation E.1, with the use of equations E.23 and E.24 yields:

$$\sigma_J^2 = \int_{-\infty}^{\infty}\int_{-\infty}^{\infty} H_I(f)H_I(-\nu)P_c(-f)P_c(\nu)\sum_{n=-\infty}^{\infty} C_n\delta(nR_q+\nu-f)H_L^I(f,\nu)d\nu df \qquad (E.25)$$

Integrating Eq. E.25 over the variable ν, we have:

$$\sigma_J^2 = \int_{-\infty}^{\infty}\sum_{n=-\infty}^{\infty} C_n H_I(f)H_I(nR_q-f)P_c(-f)P_c(f-nR_q)H_L^I(f,f-nR_q)df \qquad (E.26)$$

From equation E.24, $H_L^I(f,f-nR_q)$ can be seen to become:

$$H_L^I(f,f-nR_q) = \int_{-\infty}^{\infty} H_L(u)H_L(nR_q-u)[S_c(f+f_0-u)+S_c(f-f_0-u)]du \qquad (E.27)$$

so that finally

$$\sigma_J^2 = \sum_{n=-\infty}^{\infty} C_n \int_{-\infty}^{\infty} H_I(f)H_I(nR_q-f)P_c(-f)P_c(f-nR_q)\cdot \int_{-\infty}^{\infty} H_L(u)H_L(nR_q-u)[S_c(f+f_0-u)+S_c(f-f_0-u)]dudf \qquad (E.28)$$

APPENDIX F

THE EXPONENTIAL FOURIER SERIES OF $q_s(t)$ AND AVERAGE POWER OF THE PULSED JAMMER.

Given $q_s(t)$ as defined in Chapter II, part C and re-illustrated as shown in Figure F.1 since $q_s(t)$ is a periodic signal, it is possible to expand $q_s(t)$ in terms of an exponential Fourier series with coefficients C_n, where:

$$C_n = \frac{1}{T_q}\left[\int_0^{\rho T_q} A^2 e^{j2\pi nt/T_q}\,dt + \int_{\rho T_q}^{T_q} c^2 e^{j2\pi nt/T_q}\,dt\right] \qquad (F.1)$$

Let $t_1 = t - \frac{\rho T_q}{2}$ in the first integral and let $t_2 = t - \frac{(1+\rho)T_q}{2}$ in the second integral, so that

$$C_n = \frac{1}{T_q}\int_{-\rho\frac{T_q}{2}}^{\rho\frac{T_q}{2}} A^2 e^{j2\pi n(t_1+\rho\frac{T_q}{2})/T_q}\,dt_1 + \frac{1}{T_q}\int_{-(1-\rho)T_q/2}^{(1-\rho)T_q/2} c^2 e^{j2\pi n(t_2+\frac{T_q(1+\rho)}{2})/T_q}\,dt_2 \qquad (F.2)$$

Using properties of even and odd functions it is possible to simplify Eq. F.2 to yield

$$\begin{aligned} C_n &= \frac{1}{T_q}\left[2A^2 e^{j2\pi n\rho/2}\int_0^{\rho\frac{T_q}{2}} \cos\frac{2n\pi t_1}{T_q}dt_1 + 2C^2 e^{j2\pi n(1+\rho)/2}\int_0^{(1-\rho)\frac{T_q}{2}} \cos\frac{2n\pi t_2}{T_q}dt_2\right. \\ &= \frac{1}{T_q}\left[2A^2 e^{j\frac{2\pi n\rho}{2}}\frac{\sin 2n\pi t_1/T_q}{2n\pi/T_q}\right]_0^{\frac{\rho T_q}{2}} + \frac{1}{T_q}\left[2C^2 e^{j\frac{2n\pi(1+\rho)}{2}}\frac{\sin 2n\pi t_2/T_q}{2n\pi/T_q}\right]_0^{\frac{(1-\rho)T_q}{2}} \\ &= A^2\rho\rho^{jn\pi\rho}\frac{\sin n\pi\rho}{n\pi\rho} + C^2(1-\rho)e^{jn\pi(1+\rho)}\frac{\sin n\pi(1-\rho)}{n\pi(1-\rho)} \end{aligned} \qquad (F.3)$$

From equation F.3, we observe that if $n = 0$, then

$$C_0 = A^2\rho + C^2(1-\rho) \qquad (F.4)$$

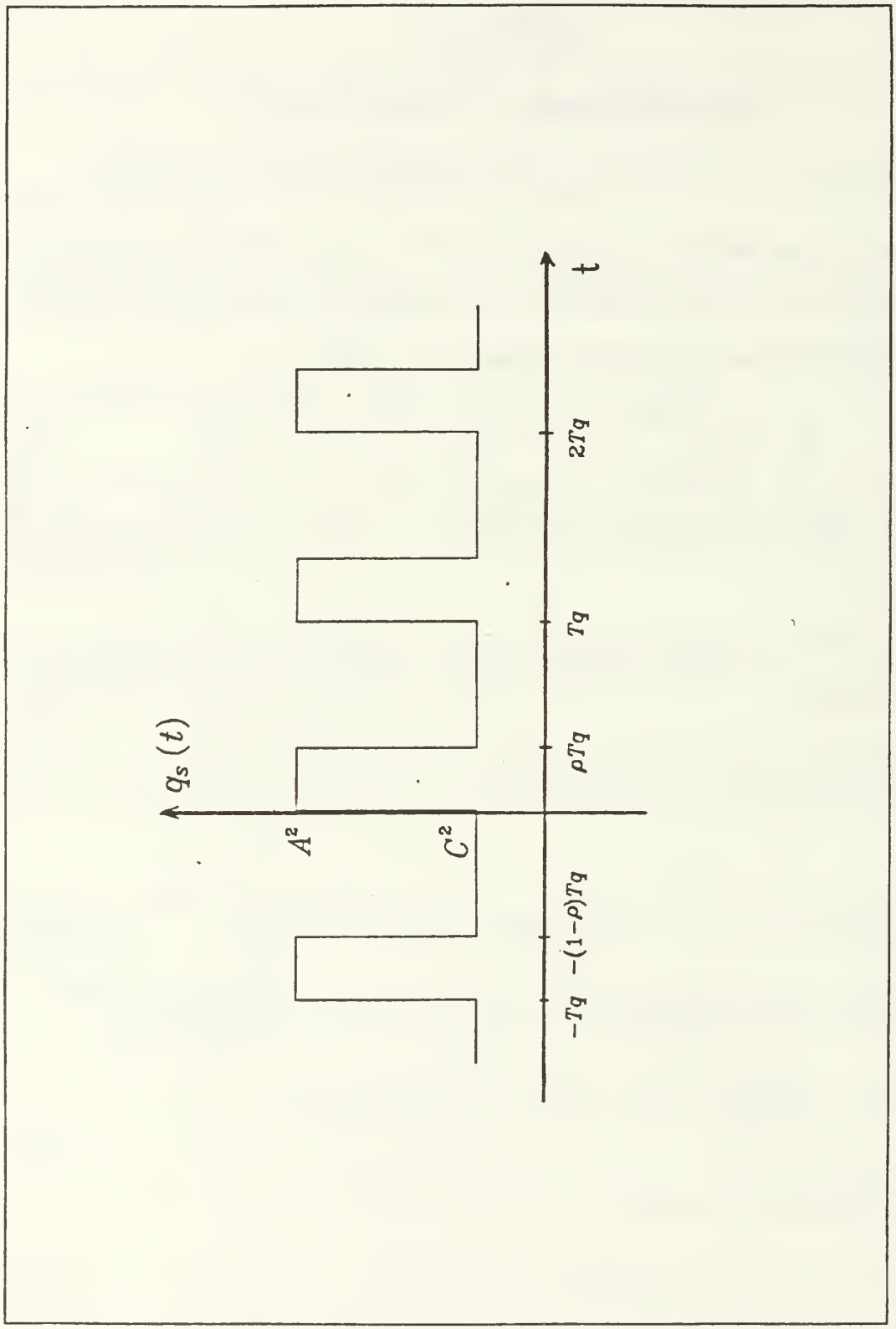

Figure F.1 Function $q_s(t)$

In the case where $n \neq 0$, C_n can be reformulated as

$$C_n = e^{jn\pi\rho}\left[A^2\rho\frac{\sin n\pi\rho}{n\pi\rho} + (-1)^n C^2(1-\rho)\frac{\sin n\pi(1-\rho)}{n\pi(1-\rho)}\right], n \neq 0 \qquad (F.5)$$

However, expanding $\sin n\pi(1-\rho)$ and taking into account that $\sin n\pi = 0$ and $\cos n\pi = (-1)^n$, the second term of equation F.5 becomes $-\rho^2 C^2 \frac{\sin n\pi\rho}{n\pi\rho}$, so that we finally obtain

$$C_n = e^{jn\pi\rho}\rho^2(A^2 - C^2)\frac{\sin n\pi\rho}{n\pi\rho} \qquad n \neq 0 \qquad (F.6)$$

Summarizing the results above, we have

$$C_n = \begin{cases} A^2\rho + C^2(1-\rho) & \text{if } n = 0 \\ \rho^2(A^2 - C^2)e^{jn\pi\rho}\frac{\sin n\pi\rho}{n\pi\rho} & \text{if } n \neq 0 \end{cases} \qquad (F.7)$$

The average power of the pulsed noise jammer can be obtained directly from the coefficients C_n. Alternatively, recall the expression for $R_y(t_1 t_2)$ from equation C.1 and let $t_1 = t_2 = t$ so that

$$R_y(t,t) = R_y(t) = 2\cos 2\pi f_0(t-t)\int_{-\infty}^{\infty} h_L(t-\alpha)h_L(t-\alpha)q_s(\alpha)d\alpha$$

or

$$R_y(t) = 2\int_{-\infty}^{\infty} h_L^2(t-\alpha)q_s(\alpha)d\alpha \qquad (F.8)$$

Assuming specifically that $h_L(t) = Be^{-Bt}U(t)$, $R_y(t)$ can be obtained as follows,

$$\begin{aligned}
R_y(t) &= 2\int_{-\infty}^{\infty} \left[Be^{-B(t-\alpha)}U(t-\alpha)\right]^2 q_s(\alpha)d\alpha \\
&= 2B^2 \int_0^{\infty} e^{-2Bx} \sum_{n=-\infty}^{\infty} C_n e^{j2\pi n(t-x)/T_q} dx \qquad \text{where } x = t-\alpha \\
&= 2B^2 \sum_{n=-\infty}^{\infty} C_n e^{j2n\pi t/t_q} \left[\frac{e^{(2B+j2n\pi/T_q)x}}{-(2B+j2\pi n/T_q)}\right]_0^{\infty} \\
&= 2B^2 \sum_{n=-\infty}^{\infty} C_n \frac{e^{j2n\pi t/T_q}}{2B+j2n\pi/T_q} \qquad (F.9) \\
&= 2B^2 \left[\frac{C_0}{2B} + \sum_{n=1}^{\infty} C_{-n} \frac{e^{j2\pi nt/T_q}}{2B-j2n\pi/T_q} + \sum_{n=1}^{\infty} C_n \frac{e^{j2\pi nt/t_q}}{2B+j2n\pi/T_q}\right] \\
&= 2B^2 \left[\frac{C_0}{2B} + 2\sum_{n=1}^{\infty} Re\left\{C_n \frac{e^{j2n\pi t/T_q}}{2B+j2\pi nT_q}\right\}\right]
\end{aligned}$$

Since the C_n coefficients have been shown to be of the form

$$C_n = e^{jn\pi\rho} f_n(A, C, \rho) \qquad (F.10)$$

Equation F.9 becomes

$$\begin{aligned}
R_y(t) &= 2B^2 \left[\frac{C_0}{2B} + 2\sum_{n=1}^{\infty} Re\left\{f_n(A,C,\rho)\frac{e^{jn\pi\rho}e^{j2n\pi t/T_q}}{2B+j2n\pi/T_q}\right\}\right] \\
&= 2B^2 \left[\frac{C_0}{2B} + 2\sum_{n=1}^{\infty} f_n(A,C,\rho) Re\left\{\frac{e^{j(n\pi\rho+2n\pi t/T_q)}}{\sqrt{(2B)^2+(2n\pi/T_q)^2}\,e^{j\tan^{-1}n\pi/BT_q}}\right\}\right] \\
&= 2B^2 \left[\frac{C_0}{2B} + 2\sum_{n=1}^{\infty} f_n(A,C,\rho)\frac{\cos\left(\frac{2n\pi t}{T_q} + n\pi\rho - \tan^{-1}\frac{n\pi}{nt_q}\right)}{\sqrt{(2B)^2+(2n\pi/T_q)^2}}\right] \qquad (F.10)
\end{aligned}$$

It is obvious that $R_y(t)$ is periodic in t with period T_q, since the average of a cosine signal is zero, we therefore have

$$\overline{R_y(t)} = 2B\left(\frac{C_0}{2}\right)$$

or

$$P_J = \overline{R_y(t)} = B[A^2\rho + C^2(1-\rho)] \qquad (F.11)$$

APPENDIX G

VARIANCE σ_J^2 FOR FAST JAMMER

In the case of fast jamming, the variance σ_J^2 of the jammer as demonstrated in Eq. 3.18 simplifies to the following expression

$$\sigma_J^2 = C_0 \int_{-\infty}^{\infty} |H_I(f)|^2 |P_c(f)|^2 \int_{-\infty}^{\infty} |H_L(u)|^2 S_c'(f-u) du df \qquad (G.1)$$

where

$$S_c'(x) = S_c(x + f_0) + S_c(x - f_0)$$

In order to simplify the notation, denote the Fourier Transform and the inverse Fourier Transform operation by $F\{(\cdot)\}$ and $F^{-1}\{(\cdot)\}$ respectively and let $*$ denote the convolution operation. Define

$$v(t) \triangleq F^{-1}\{V(f)\} \qquad (G.2)$$

where

$$V(f) = \int_{-\infty}^{\infty} |H_L(u)|^2 S_c'(f-u) du \qquad (G.3)$$

so that σ_J^2 can be reformulated as follows

$$\begin{aligned} \sigma_J^2 &= C_0 \int_{-\infty}^{\infty} |H_I(f)|^2 |P_c(f)|^2 V(f) df \\ & C_0 \int_{-\infty}^{\infty} |H_I(f)|^2 |P_c(f)|^2 \int_{-\infty}^{\infty} v(t) e^{-j2\pi ft} dt \; df \\ &= C_0 \int_{-\infty}^{\infty} v(t) \int_{-\infty}^{\infty} |H_I(f)|^2 |P_c(f)|^2 e^{-j2\pi ft} dt \; df \\ &= C_0 \int_{-\infty}^{\infty} v(t) F^{-1}\left\{ |H_I(f)|^2 |P_c(f)|^2 \right\} dt \end{aligned} \qquad (G.4)$$

Recall from Chap. III, Eq. 3.17 that:

$$P_c(f) = G(f - f_0) + G(f + f_0)$$

$$G(f) = \frac{T_b}{2}\text{sinc}\,(fT_b)e^{-j2\pi fT_b}$$

where for reasonable values of f_0 and T_b

$$|P_c(f)|^2 = P_c(f)P_c(-f) \approx |G(f - f_0)|^2 + |G(f + f_0)|^2 \qquad (G.5)$$

or equivalently

$$|P_c(f)|^2 = \left(\frac{T_b}{2}\right)^2 \text{sinc}^2(f - f_0)T_b + \left(\frac{T_b}{2}\right)^2 \text{sinc}^2(f + f_0)T_b \qquad (G.6)$$

The inverse Fourier Transform of this function can be easily obtained from tables (see Ref. 9), namely

$$F^{-1}\left\{|P_c(f)|^2\right\} = \frac{T_b}{4}\Lambda\left(\frac{t}{T_b}\right)\left(e^{j2\pi f_0 t} + e^{-j2\pi f_0 t}\right) \qquad (G.7)$$

where

$$\Lambda\left(\frac{t}{T_b}\right) = \begin{cases} 1 - \dfrac{|t|}{T_b} & \text{if} \quad |t| \le T_b \\ 0 & \text{if} \quad |t| > T_b \end{cases}$$

The same considerations apply for $|H_I(f)|^2$ since $H_I(f)$ is the bandpass filter transfer function specified in terms of shifted lowpass equivalents. Since $H_I(f)$ is significant for $f = \pm f_0$ over a restricted frequency band,

$$|H_I(f)|^2 \approx |H_{Lb}(f - f_0)|^2 + |H_{Lb}(-f - f_0)|^2 \qquad (G.8)$$

where the lowpass equivalent $H_{Lb}(f)$ is given by

$$H_{Lb}(f) = \frac{b}{b + j2\pi f} \qquad (G.9)$$

so that

$$|H_{Lb}(f)|^2 = \frac{b}{2}\left(\frac{2b}{b^2 + (2\pi f)^2}\right) \qquad (G.10)$$

Consequently,

$$F^{-1}\left\{|H_I(f)|^2\right\} = \frac{b}{2}e^{-b|t|}\left[e^{j2\pi f_0 t} + e^{-j2\pi f_0 t}\right] \tag{G.11}$$

so that evaluation of $F^{-1}\left\{|H_I(f)|^2|P_c(f)|^2\right\}$ can be accomplished by using the convolution theorem [Ref. 9], that is

$$\begin{aligned}
F^{-1}\left\{|H_I(f)|^2|P_c(f)|^2\right\} &= F^{-1}\left\{|H_I(f)|^2\right\} * F^{-1}\left\{|P_c(f)|^2\right\} \\
&= \int_{-\infty}^{\infty} \frac{bT_b}{8}\Lambda\left(\frac{\tau}{T_b}\right)\left(e^{j2\pi f_0\tau} + e^{-j2\pi f_0\tau}\right)e^{-b|t-\tau|}\left(e^{j2\pi f_0(t-\tau)} + e^{-j2\pi f_0(t-\tau)}\right)d\tau \\
&= \frac{bT_b}{8}\int_{-\infty}^{\infty} e^{-b|t-\tau|}\Lambda\left(\frac{\tau}{T_b}\right)\cos 2\pi f_0(t-\tau)d\tau \\
&= \frac{bT_b}{8}\int_{-\infty}^{\infty} e^{-b|t-\tau|}\Lambda\left(\frac{\tau}{T_b}\right)g(t,\tau)d\tau
\end{aligned} \tag{G.12}$$

where

$$\begin{aligned}
g(t,\tau) &= \cos 2\pi f_0\tau\cos 2\pi f_0(t-\tau) \\
&= \frac{1}{2}\left[\cos 2\pi f_0 t + \cos 2\pi f_0 t\cos 4\pi f_0\tau + \sin 2\pi f_0 t\sin 4\pi f_0\tau\right]
\end{aligned} \tag{G.13}$$

According to the value of $|t-\tau|$, Eq. G.12 can be further expressed as follows:

$$F^{-1}\left\{|H_I(f)|^2\cdot|P_c(f)|^2\right\} = I_1 + I_2 \tag{G.14}$$

where:

$$I_1 = \frac{bT_b}{8}\int_{-\infty}^{t} e^{-b(t-\tau)}\Lambda\left(\frac{\tau}{T_b}\right)g(t,\tau)d\tau \tag{G.15}$$

$$I_2 = \frac{bT_b}{8}\int_{t}^{\infty} e^{-b(\tau-t)}\Lambda\left(\frac{\tau}{T_b}\right)g(t,\tau)d\tau \tag{G.16}$$

We can now proceed to the specification of $v(t)$ which is obtained from

$$\begin{aligned}
v(t) &= F^{-1}\left\{\int_{-\infty}^{\infty}|H_L(u)|^2\cdot S_c'(f-u)du\right\} \\
&= F^{-1}\left\{|H_L(f)|^2\right\}\cdot F^{-1}\left\{S_c(f)\right\} \\
&= Be^{-B|t|}\Lambda\left(\frac{t}{T_c}\right)\cos 2\pi f_0 t
\end{aligned} \tag{G.17}$$

since

$$F^{-1}\{|H_L(f)|^2\} = Be^{-B|t|}\cos 2\pi f_o t \qquad (G.18)$$

Substituting Eq. G.4 with Eq. G.14 and G.17 yields

$$\sigma_J^2 = C_0 B \int_{-\infty}^{\infty} e^{-B|t|}\Lambda\left(\frac{t}{T_c}\right)\cos 2\pi f_0 t(I_1 + I_2)dt$$

The limit of integration can be reduced to the interval $[-T_c, T_c]$ since the function $\Lambda\pi f_0 t(I_1 + I_2)dt$ The limit of integration can be reduced to the interval $[-T_c, T_c]$ since the function $\Lambda\left(\frac{t}{T_c}\right)$ is zero except for $|t| \leq T_c$, hence

$$\sigma_J^2 = BC_0 \int_{-t_c}^{T_c} e^{-B|t|}\Lambda\left(\frac{t}{T_c}\right)\cos 2\pi f_0 t(I_1 + I_2)dt \qquad (G.19)$$

According to the value of t, two cases can be considered as follows:

Case (1) $T_b > t > 0$,

In this case, we have

$$I_1 + I_2 = \frac{bT_b}{8}\left[\int_{-T_b}^{0} e^{-b(t-\tau)}\left(1 + \frac{\tau}{T_b}\right)g(t,\tau)d\tau + \int_0^t e^{-b(t-\tau)}\left(1 - \frac{\tau}{T_b}\right)g(t,\tau)d\tau + \int_t^{T_b} e^{-b(\tau-t)}\left(1 - \frac{\tau}{T_b}\right)g(t,\tau)d\tau\right] \qquad (G.20)$$

Since Eq. G.13 shows that $g(t,\tau)$ is a function of $\cos 4\pi f_0\tau$ and $\sin 4\pi f_0\tau$, it can be seen that the integration of functions of the form $e^{m\tau}\cos 4\pi f_0\tau$ and $e^{m\tau}\sin 4\pi f_0\tau$, as well as forms $te^{m\tau}\cos 4\pi f_0\tau$ and $te^{m\tau}\sin 4\pi f_0 t$ will yield terms involving the factors $(m^2 + 16\pi^2 f_0^2)$ and $(m^2 + 16\pi^2 f_0^2)^2$ in the denominator of the result while the numerators remain bounded. The numerators are proportional to m, which in this case equals b or B. Since in a practical system,

$$f >> b \quad \text{and} \quad f_0 >> B.$$

the contribution of the corresponding terms are therefore not significant, so that, Eq G.20 can be simplified as follows:

$$I_1 + I_2 \approx \frac{bT_b}{8} \cdot \frac{1}{2} \cos 2\pi f_0 t \left[e^{-bt} \int_{-T_b}^{0} e^{b\tau} \left(1 + \frac{\tau}{T_b}\right) d\tau + \right.$$

$$\left. e^{-bt} \int_{0}^{t} \Rightarrow e^{b\tau} \left(1 - \frac{\tau}{T_b}\right) d\tau + e^{bt} \int_{t}^{T_b} e^{-b\tau} \left(1 - \frac{\tau}{T_b}\right) d\tau \right] \qquad (G.21)$$

Eq. G.21 can be evaluated by using standard mathematics tables [Ref. 10] and therefore

$$I_1 + I_2 \approx \frac{bT_b}{8} \cos 2\pi f_0 t \left[\frac{1}{b} - \frac{t}{bT_b} - \frac{e^{bt}}{b^2 T_b} + \frac{e^{-bT_b}}{2b^2 T_b} \left(e^{-bt} + e^{bt}\right) \right]. \qquad (G.22)$$

Case (2) $0 > t > -T_b$,

In this case we have

$$I_1 + I_2 = \frac{bT_b}{8} \left[\int_{-T_b}^{t} e^{-b(t-\tau)} \left(1 + \frac{\tau}{T_b}\right) g(t,\tau) + \int_{t}^{0} e^{-b(\tau - t)} \left(1 + \frac{\tau}{T_b}\right) g(t,\tau) d\tau \right.$$
$$\left. + \int_{0}^{T_b} e^{-b(\tau - t} \left(1 - \frac{\tau}{T_b}\right) g(t,\tau) d\tau \right] \qquad (G.23)$$

By considerations similar to those presented in Case (1), Eq. G.23 can be approximated by

$$I_1 + I_2 \approx \frac{bT_b}{8} \cdot \frac{1}{2} \cos 2\pi f_0 t \left[e^{-bt} \int_{-T_b}^{t} e^{b\tau} \left(1 + \frac{\tau}{T_b}\right) d\tau + e^{bt} \int_{t}^{0} e^{-b\tau} \left(1 + \frac{\tau}{T_b}\right) d\tau \right.$$
$$\left. + e^{bt} \int_{0}^{T_b} e^{-b\tau} \left(1 - \frac{\tau}{T_b}\right) d\tau \right] \qquad (G.24)$$

so that

$$I_1 + I_2 \approx \frac{bT_b}{8} \cos 2\pi f_0 t \left[\frac{1}{b} + \frac{t}{bT_b} - \frac{e^{bt}}{b^2 T_b} + \frac{e^{-bT_b}}{2b^2 T_b} \left(e^{-bt} + e^{bt}\right) \right] \qquad (G.25)$$

We can now proceed to the evaluation of σ_J^2 expressed by Eq. G.19 according to the range of t. Since $T_c < T_b$,

$$\sigma_J^2 = \frac{BC_0bT_b}{8}\int_{-T_c}^{0} e^{Bt}\left(1+\frac{t}{T_c}\right)\cos^2 2\pi f_0 t\left[\frac{1}{b}+\frac{t}{bT_b}-\frac{e^{bt}}{b^2T_b}+\frac{e^{-bT}}{2b^2T_b}\left(e^{-bt}+e^{bt}\right)\right]dt$$
$$+\frac{BC_0bT_b}{8}\int_{0}^{T_c} e^{-Bt}\left(1-\frac{t}{t_c}\right)\cos^2 2\pi f_0 t\left[\frac{1}{b}-\frac{t}{bT_b}-\frac{e^{bt}}{b^2T_b}+\frac{e^{-bT_b}}{2b^2T_b}\left(e^{-bt}+e^{bt}\right)\right]dt \qquad (G.26)$$

and using $\cos^2 2\pi f_0 t = \frac{1}{2}(\cos 4\pi f_0 t + 1)$ the reasoning that gave rise to the simplifications in evaluating Eq. G.20 can be used here to neglect the terms involving $(m^2 + 16\pi^2 f_0^2)$ or $(m^2 + 16\pi^2 f_0^2)^2$ in the denominator. Thus Eq. G.26 can be further simplified as follows:

$$\sigma_J^2 = \frac{BC_0bT_b}{16}\left\{\int_{-T_c}^{0} e^{Bt}\left(1+\frac{t}{T_c}\right)\left[\frac{1}{b}+\frac{t}{bT_b}-\frac{e^{bt}}{b^2T_b}+\frac{e^{-bT_b}}{2b^2T_b}\left(e^{-bt}+e^{bt}\right)\right]dt\right.$$
$$\left.+\int_{0}^{T_c} e^{-Bt}\left(1-\frac{t}{T_c}\right)\left[\frac{1}{b}-\frac{t}{bT_c}-\frac{e^{bt}}{b^2T_b}+\frac{e^{-bT_b}}{2b^2T_b}\left(e^{-bt}+e^{bt}\right)\right]dt\right\} \qquad (G.27)$$

and using standard mathematics tables (Ref. 10) results in

$$\sigma_J^2 = \frac{B_0C_0bT_b}{8}\left\{\frac{1}{b}\left[\frac{1}{B}-\frac{1}{B^2T_c}\left(1-e^{-BT_c}\right)\right]+\frac{1}{bT_b}\left[\frac{2}{B^3T_c}\left(1-e^{-BT_c}\right)\right.\right.$$
$$-\frac{1}{B^2}\left(1+e^{-BT_c}\right)\Big]-\frac{1}{b^2T_b}\left[\frac{e^{-BT_c}e^{bT_c}}{2(B-b)^2T_c}+\frac{e^{-BT_c}e^{-bT_c}}{2(B+b)^2T_c}\right.$$
$$\left.+\frac{B}{B^2-b^2}-\frac{B^2+b^2}{(B^2-b^2)^2T_c}\right]+\frac{e^{-bT_b}}{b^2T_b}\left[\frac{2B}{B^2-b^2}-\frac{2(B^2+b^2)}{(B^2-b^2)^2T_c}\right. \qquad (G.28)$$
$$\left.\left.+\frac{e^{-(B-b)T_c}}{(b-B)^2T_c}+\frac{e^{-(B+b)T_c}}{(B+b)^2T_c}\right]\right\}$$

which by regrouping terms, obtains the final form

$$\sigma_J^2 = \frac{C_0T_b}{8}\left\{1+\left(\frac{2}{B^2T_bT_c}-\frac{1}{BT_c}\right)\left(1-e^{-BT_c}\right)-\frac{1+e^{-BT_c}}{BT_b}\right.$$
$$+\left(2e^{-bT_b}-1\right)\left[\frac{B^2}{bT_b(B^2-b^2)}-\frac{B(B^2+b^2)}{bT_bT_c(B^2-b^2)^2}\right. \qquad (G.29)$$
$$\left.\left.+\frac{Be^{-BT_c}e^{-bT_c}}{2bT_bT_c(B+b)^2}+\frac{Be^{-BT_c}e^{bT_c}}{2bT_bT_c(B-b)^2}\right]\right\}$$

APPENDIX H

STATISTICS OF Y_J AND N_{th}

We first recall the definitions of N_{th} and Y_J from Chapter IV as follows

$$Y_J \triangleq \int_0^{T_b} y(t)c(t) * h_I(t) \cos 2\pi f_o t dt \tag{H.1}$$

$$N_{th} \triangleq \int_0^{T_b} N_{th}(t)c(t) * h_I(t) \cos 2\pi f_o t dt \tag{H.2}$$

Observe that Y_J is a zero mean random variable since the jammer and the spreading code $c(t)$ are assumed uncorrelated and furthermore, $c(t)$ has zero mean. The variance σ_J^2 of Y_J has been developed in Chap. 3 and can be expressed as (see Eq. 3.19)

$$\begin{aligned}\sigma_J^2 = \frac{C_0 T_b}{8}\Bigg\{1 + (1 - e^{-BT_c})\left(\frac{2}{B^2 T_b T_c} - \frac{1}{BT_c}\right) - \frac{1 + e^{-BT_c}}{BT_b} \\ + (2e^{-bT_b} - 1)\left[\frac{B^2}{bT_b(B^2 - b^2)} - \frac{B(B^2 + b^2)}{bT_b T_c (B^2 - b^2)^2}\right. \\ \left. + \frac{Be^{-BT_c}e^{-bT_c}}{2bT_b T_c (B + b)^2} + \frac{Be^{-BT_c}e^{bT_c}}{2bT_b T_c (B - b)^2}\right]\Bigg\}\end{aligned} \tag{H.3}$$

Replacing now B and b in Eq. H.3 by $2\pi R_c$ and $2\pi R_b$ respectively thereby setting the 3 dB cutoff of the filters appropriately, with

$$G_c \triangleq \frac{R_c}{R_b}$$

defined as the processing gain, a final expression for σ_J^2 is obtained as follows

$$\sigma_J^2 = \frac{C_o T_b}{8} J(G_c) \tag{H.4}$$

where

$$\begin{aligned}J(G_c) = 1 + \frac{(1 - e^{-2\pi})(1 - \pi G_c)}{2\pi^2 G_c} - \frac{1 + e^{-2\pi}}{2\pi G_c} + \frac{G_c^2(2e^{-2\pi} - 1)}{2\pi}\Bigg\{\frac{1}{G_c^2 - 1} \\ - \frac{G_c^2 + 1}{2\pi(G_c^2 - 1)^2} + \frac{e^{-2\pi}}{4\pi}\left[\frac{e^{-\frac{2\pi}{G_c}}}{(G_c + 1)^2} + \frac{e^{\frac{2\pi}{G_c}}}{(G_c - 1)^2}\right]\Bigg\}\end{aligned} \tag{H.5}$$

The determination of the variance σ_{th}^{e} of the random variable N_{th} can be accomplished in a manner very similar to that used in the determination of σ_J^2. Observing however that replacing in the jammer model the deterministic priodic signal $q(t)$ with a constant unit amplitude function, namely $q(t) = 1$, setting $R_W(t_1, t_2)$ equal to $\frac{N_o}{2}\delta(t_2, t_1)$ (see Eqs. 2.16 and 2.17) results in a simple AWGN noise model having PSD level $N_o/2$. Thus all evaluations involving the jammer can now be used with the stated modificiations in order to characterize the noise contributions to the performance of the system. Therefore, (see Eq. E.13)

$$\eta(\tau, \gamma) = \int_{-\infty}^{\infty} h_L(\tau - \alpha) h_L(\gamma - \alpha) d\alpha \tag{H.5}$$

and with

$$h_L(t) = Be^{-Bt}U(t)$$

then

$$\begin{aligned} \eta(\tau, \gamma) &= B^2 e^{-B\tau} e^{-B\gamma} \int_{-\infty}^{\mathrm{Min}(\tau,\gamma)} e^{2B\alpha} d\alpha \\ &= \frac{B}{2} e^{-B|\tau - \gamma|} \end{aligned} \tag{H.6}$$

Thus, the auto correlation function $R_n(t, \tau)$ of the noise $N_{th}(t)$ is

$$R_n(t, \tau) = \frac{N_o}{2} B e^{-B|\tau - \gamma|} \cos 2\pi f_o(\tau - \gamma) \tag{H.7}$$

From the methodology of Chap. 3, Eq. E.14 becomes

$$H(u, w) = \int_{-\infty}^{\infty} \int_{-\infty}^{\infty} N_o \frac{B}{2} e^{-B|\tau - \gamma|} e^{-j2\pi\tau u} e^{j2\pi\gamma w} d\tau d\gamma \tag{H.8}$$

Evaluation of Eq. H.8 can be shown to yield

$$H(u, w) = N_o \frac{B}{2} \left\{ \frac{1}{B - j2\pi u} + \frac{1}{B + j2\pi u} \right\} \delta(u - w) \tag{H.9}$$

Therefore, the variance σ_{th}^2 of N_{th} (see Eq. E.25)

$$\sigma_{th}^2 = \int_{-\infty}^{\infty}\int_{-\infty}^{\infty} \frac{N_o}{2} H_I(f)H_I(-\nu)P_c(-f)P_c(-\nu) \int_{-\infty}^{\infty} H(u, u+\nu-f)[S_c(f-u+f_o)+S_c(f-u+f_o)]dudfd\nu \tag{H.10}$$

where

$$\begin{aligned} H(u, u+\nu-f) &= N_o\frac{B}{2}\left\{\frac{2B}{B^2+(2\pi u)^2}\right\}\delta(u-(u+\nu-f)\cdot \\ &= N_o\frac{B}{2}\left\{\frac{2B}{B^2+(2\pi u^2)^2}\right\}\delta(f-\nu) \end{aligned} \tag{H.11}$$

Letting $f = \nu - f_o$ or $f = \nu + f_o$ as appropriate in the two integrals, obtain

$$\sigma_{th}^2 = \int_{-\infty}^{\infty} N_o|H_I(f+f_o)P_c(f+f_o)|^2 Z(f)df + \int_{-\infty}^{\infty} N_o|H_I(f-f_o)P_c(f-f_o)|^2 Z(f)df \tag{H.12}$$

where

$$Z(f) = \int_{-\infty}^{\infty} \frac{B}{2}\frac{2B}{B^2+(2\pi u)^2} S_c(f-u)dudf \tag{H.13}$$

$Z(f)$ can be evaluated further as follows

$$\begin{aligned} Z(f) &= \frac{B}{2}\frac{2B}{B^2(2\pi f)^2} * S_c(f) = \frac{B}{2}F\left\{e^{-B|t|}\cdot R_c(t)\right\} \\ &= \frac{B}{2}\int_{-\infty}^{\infty} e^{-B(t)}R_c(t)e^{-j2\pi ft}dt \\ &= B\left[\int_0^{T_c} e^{-Bt}\cos 2\pi ftdt - \int_o^{T_c} e^{-Bt}\frac{t}{T_c}\cos 2\pi ftdt\right] \end{aligned} \tag{H.14}$$

The two integrals in Eq. H.14 can be evaluated separately and with $BT_c = 2\pi$, we have

$$Z(f) = \frac{1}{2\pi}Z'(f)$$

where

$$Z'(f) = \frac{1}{[1+(fT_c)^2]^2}\left[\left(e^{-2\pi}\cos 2\pi fT_c - 1\right)\left((fT_c)^2-1\right) - 2fT_c\sin 2\pi fT_c\right] \tag{H.15}$$

From Figure H.1, it can be observed that if $R_b << R_c$, then $Z'(f) \approx 1$ for f within the interval $[-R_b, R_b]$. In fact, $Z(f)$ is significant only for $|f| << R_b$. Hence, Eq. H.12 can be simplified as follows:

$$\sigma_{th}^2 \approx \frac{N_o}{2\pi}\left[\int_{-R_b}^{R_b} |H_I(f+f_o)P_c(f+f_o)|^2 df + \int_{-R_b}^{R_b} |H_I(f-f_o)P_c(f-f_o)|^2 df\right]$$
$$= \frac{N_o}{\pi}\int_{-R_b}^{R_b} |H_I(f-f_o)P_c(f-f_o)|^2 df \qquad (H.16)$$

From Eq. G.6, we have

$$|P_c(f-f_o)|^2 \approx |G(f-f-2f_o)|^2 + |G(f)|^2$$

where

$$G(f) = \left(\frac{T_b}{2}\right)^2 \text{sinc}^2 fT_b. \qquad (H.17)$$

The term $|G(f-2f_o)|$ has significant components outside the integration region $[-R_b, R_b]$. Furthermore from Eq. G.8

$$|H_I(f-f_o)|^2 \approx |H_{L_b}(f-2f_o)|^2 + |H_{L_b}(-f)|^2$$

and again, the term $|H_{L_b}(f-2f_o)|$ can be dropped from further consideration due to reasons similar to those discussed above in the context of $|G(f-2f_o)|$. Thus

$$\sigma_{th}^2 \approx \frac{N_o}{\pi}\int_{-R_b}^{R_b} |H_{L_b}(f)|^2 \left(\frac{T_b}{2}\right)^2 \text{sinc}^2 fT_b\, df$$

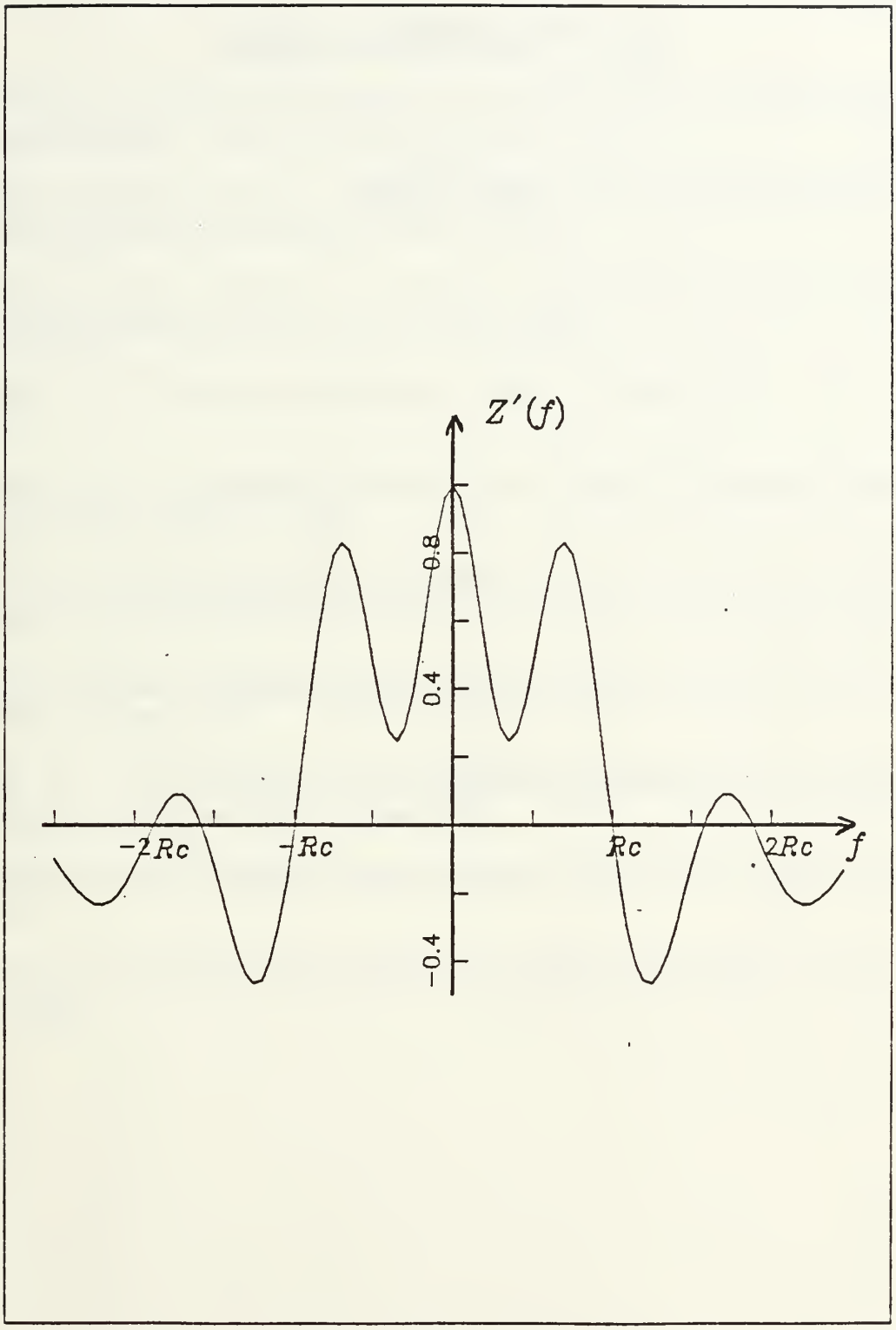

Figure H.1 Function Z′(f)

and since $|H_{L_b}(f)|^2$ has 3 dB cutoff at $f = \pm R_b$, the integral itself can be approximated by

$$\frac{1}{2R_b}\int_{-R_b}^{R_b} \text{sinc}^2(fT_b)df \approx k = 0.903$$

Finally

$$\sigma_{th}^2 \approx \frac{N_o T_b}{2\pi} k \qquad (H.18)$$

LIST OF REFERENCES

1. Simon, M. K., Omura, J. K., Scholtz, R. A., and Levitt, B. K., Spread Spectrum Communications, Computer Science Press, Inc., 1985,

2. Ziemer, R. E., Peterson, R. L., Digital Communications and Spread Spectrum Systems, Macmillan Publishing Company, 1985.

3. Cattermole, K. W., O'Reilly, J. J., Problems of Randomness in Communication Engineering, Wiley-Interscience, New York, 1984.

4. Whalen, A. D., Detection of Signals in Noise, Academic Press, New York, 1971.

5. Helstrom, C. W., Probability and Stochastic Processes for Engineers, Macmillan Publishing Company, 1984.

6. Brown, R. G., Introduction to Radom Signal Analysis and Kalman Filtering, John Wiley & Sons, 1983.

7. Peebles, Peyton Z., Communication System Principles, Addison-Wesley Publishing Company, 1982.

8. Ricci, F. J., and Schutzer, D., U.S. Military Communications - A C^3I Force Multiplier, Computer Science Press, 1986.

9. Brigham, Oran E., The Fast Fourier Transform, Prentice-Hall, Englewood Cliffs, 1974.

10. Beyer, W. H., CRC Standard Mathematical Tables, 27^{th} Edition, CRC Press, Inc., 1985.

INITIAL DISTRIBUTION LIST

	No. Copies
1. Defense Technical Information Center Cameron Station Alexandria, Virginia 22304-6145	2
2. Library, Code 0142 Naval Postgraduate School Monterey, California 93943-5002	2
3. Department Chairman, Code 62 Department of Electrical and Computer Engineering Naval Postgraduate School Monterey, California 93943	1
4. Professor D. Bukofzer, Code 62Bh Department of Electrical and Computer Engineering Naval Postgraduate School Monterey, California 93943	5
5. Professor Glen A. Myers; Code 62Mv Department of Electrical and Computer Engineering Naval Postgraduate School Monterey, California 93943	1
6. DD COMMS Defense Material Organization Ministry of Defense, Singapore COMMUNICATIONS DIVISION PAYA LEBAR AIRPORT SINGAPORE 1953 Republic of Singapore	4
7. Mr. Low Kah Meng Blk. 6, #04-168 REDHILL CLOSE Singapore 0315 Republic of Singapore	2

DUDLEY KNOX LIBRARY
NAVAL POSTGRADUATE SCHOOL
MONTEREY, CALIFORNIA 93943-5002

Thesis
L8545 Low
c.1 Representation of non-stationary narrowband random processes and their application and effectiveness as jamming signals in spread spectrum communication system.

26 SEP 88 80088
26 SEP 88 80088
26 SEP 88 80088
28 SEP 89 80164

Thesis
L8545 Low
c.1 Representation of non-stationary narrowband random processes and their application and effectiveness as jamming signals in spread spectrum communication system.

thesL8545
Representation of nonstationary narrowba
3 2768 000 72703 6
DUDLEY KNOX LIBRARY